2022-12-29

On the Effective Stiffness of Slender Concrete Masonry Walls

Bogoslavov, Mihailo

UNIVERSITY OF CALGARY

On the Effective Stiffness of Slender Concrete Masonry Walls

by

Mihailo Bogoslavov

A THESIS

SUBMITTED TO THE FACULTY OF GRADUATE STUDIES

IN PARTIAL FULFILMENT OF THE REQUIREMENTS FOR THE

DEGREE OF MASTER OF SCIENCE

GRADUATE PROGRAM IN CIVIL ENGINEERING

CALGARY, ALBERTA

DECEMBER, 2022

Abstract

The slender masonry wall design procedure in the Canadian Standard for Design of Masonry Structures, CSA S304-14, (2014) has been found to be overly conservative. The calculated effective stiffness term, EI_{eff}, which is used to determine the secondary moment due to wall deflection, was noted as a potentially significant cause of this conservatism. In this thesis, the degree to which the effective stiffness term contributes as a source of error is assessed by analyzing the results from a concrete block wall testing program (Hatzinikolas et al., 1978a) and comparing the recorded lateral wall deflections to the deflections calculated as per CSA S304-14 (2014). The effective stiffness is shown to be particularly underestimated by the procedure in the Standard (leading to overdesign of walls) when a wall is designed to be loaded at a low axial load eccentricity. A more accurate equation for calculating the effective stiffness of a wall as it is being loaded is developed and recommended in this thesis, whereby the effective stiffness depends on the wall's thickness, critical buckling load and the applied axial load and its eccentricity. A discrepancy between the expected and observed failure modes of slender walls loaded at low axial load eccentricities is noted in the analysis, whereby slender masonry walls commonly experience compressive material failure when loaded at a low axial load eccentricity, even though slenderness effects are expected to contribute to out-of-plane failure. A potential alternative design procedure template is presented, whereby a wall is first categorized based on its expected failure mode and only then designed either as a wall which is expected to experience slenderness effects (a wall expected to deflect significantly and experience out-of-plane failure) or a wall for which slenderness effects need not be considered because it will likely experience material failure and not deflect much laterally (despite the fact that it would be currently categorized as slender by CSA S304-14 (2014) based on its slenderness ratio).

Acknowledgements

My supervising professor, Dr. Nigel Shrive, has shown me immense support, kindness and patience, for which I feel deeply indebted. His curiosity and passion for our vocation were inspirational and stimulated a creative and immensely positive atmosphere within our research group. I would like to thank our whole research group for their encouragement and advice, but particularly Dr. Andrea Isfeld, Maithree Kurukulasuriya, Hasini Rathnayake, Ahmed Ahmed, George Iskander and Baher Haleem for their valuable suggestions and detailed discussions.

I would like to express my gratitude to the examining committee, Dr. Ron Wong and Dr. Les Sudak, for the time they have taken to review this thesis and for their valuable input.

I am thankful to the University of Calgary for facilitating this research and for the opportunities I was provided.

My wife, Elitsa, supported me tirelessly throughout my studies, as did our whole family and many close friends, for which I am most grateful.

In memory of my mother, Sonja

Table of Contents

List of Tables

List of Figures

Chapter 1: Thesis Overview

1.1 Introduction

Representatives of the masonry industry across Canada (i.e., the Alberta Masonry Council (2020) and the Canadian Masonry Design Centre (2020)) have identified a trend of the masonry industry losing out to competitors due to masonry construction becoming increasingly economically uncompetitive relative to other materials used under common design and site conditions. This was particularly the case in applications requiring the construction of tall walls, with prefabricated concrete tilt-up walls and wood stud walls being used in place of masonry block walls, as per the Alberta Masonry Council (2020) and Canadian Wood Council (2000). Researchers at the University of Calgary, most notably in the works of Müller et al. (2017) and Isfeld et al. (2019), have identified the sections of the Canadian Standard for the Design of Masonry Structures, CSA S304-14, (2014) relating to the design of slender masonry walls as a particular concern due to the overly conservative design prescriptions. The purpose of this thesis is to examine the procedure for the design of slender masonry walls in the Canadian Standard for the Design of Masonry Structures, CSA S304-14, (2014) in order to quantitatively assess its accuracy as a design prescription and to establish a theoretical foundation for the development of a more rational design approach to achieve more safe and elegant designs.

1.2 The Canadian Standard for the Design of Masonry Structures as It Relates to Slender Walls

In the design procedure for masonry walls, the Canadian Standard, CSA S304-14, (2014) differentiates walls based on their slenderness ratio (effective height to thickness ratio, kh/t), identifying walls for which the effects of slenderness must be considered. Slenderness is defined to differentiate walls which will experience significant second order moment effects. While the primary moment develops from the eccentricity of the axial load as applied to the wall (or from otherwise induced moment), the secondary moment develops from the applied axial load acting over the initial lateral displacement of the wall as it deforms horizontally and further amplifies the moment from initial axial load. Walls which exceed the slenderness ratio for which the effect of slenderness must be considered are expected to experience out-of-plane failure, while short walls are expected to experience material failure when loaded under compression. As per the Standard (2014), slenderness is to be considered when:

$$kh/t \geq (10 - 3.5\left(\frac{e_1}{e_2}\right)) \tag{1.1}$$

where e_1 and e_2 represent the top and bottom wall applied axial load eccentricities.

The Standard (2014) further differentiates between two categories of slender walls based on their slenderness ratios, for which the design criteria differ. For slenderness ratios equal to or greater than 30, the applied axial load must not exceed 10% of the wall's compressive strength. In both cases, the secondary moment is calculated either using the moment magnifier method or the load-displacement (Pδ) method.

The moment magnifier method is defined as (as per CSA S304-14, Clause 10.7.4.3):

$$M_{ftot} = M_{fp}\frac{C_m}{1-\frac{P_f}{P_{cr}}} \geq M_{fp} \tag{1.2}$$

where M_{ftot} represents the total moment (accounting for secondary moment), M_{fp} represents the primary moment calculated from the initial axial and lateral loads, P_f represents the initial axial load, P_{cr} represents the critical axial compressive load (as shown below):

$$P_{cr} = \pi^2\phi_{er}(EI)_{eff}/[(1 + 0.5\beta_d)(kh)^2] \tag{1.3}$$

where EI_{eff} represents the effective flexural stiffness and serves to account for the loss of wall cross-section utilized in resisting bending as the wall cracks (this term is of central importance to this thesis and will be further thoroughly discussed), β_d represents the ratio of the total factored dead load moment to total factored moment, ϕ_{er} representing the resistance factor for the member stiffness used in the determination of slenderness effects on the capacity of reinforced masonry (ϕ_{e} is used for unreinforced masonry), k represents the effective height factor and h represents the wall height. In the research presented throughout this thesis resistance factors (such as $\phi_{\mathrm{e}}, \phi_{\mathrm{er}}, \phi_{\mathrm{m}}$ and ϕ_s) were all assigned a value of 1 in order to most accurately compare experimental results with the design equation outputs from the Canadian Standard.

C_m (as it appears in Equation 1.2) represents the moment diagram factor (shape) and is defined below:

$$C_m = 0.6 + 0.4\, M_1/M_2 \geq 0.4 \quad ; \quad M_2 \geq M_1 \tag{1.4}$$

where M_2 & M_1 represent the wall top and bottom moments.

The Standard (2014) defines the load displacement method as (as per CSA S304-14, Clause 10.7.4.2):

$$M_{ftot} = M_{fp} + P_f \delta_f \tag{1.5}$$

where M_{ftot} represents the total moment (accounting for secondary moment), M_{fp} represents the primary moment calculated from the initial axial and lateral loads, δ_f represents the lateral deflection of the wall at the critical section (the deflection is to be calculated using the effective flexural stiffness term, EI_{eff}) and P_f represents the axial load applied to the wall.

The effective flexural stiffness term, EI_{eff}, is required as part of the critical axial compressive load calculation (calculated as part of the moment magnifier method procedure) as well as for the wall lateral deflection calculation (required for the load-displacement method procedure). It is calculated as follows (as per CSA S304-14, Clause 7.7.6.4 & Clause 10.7.4.4):

$$(EI)_{eff} = E_m[0.25 I_o - (0.25 I_o - \ I_{cr})(\frac{e - e_k}{2 e_k})] \leq 0.25 E_m I_o$$

but $\geq E_m I_{cr}$ for reinforced walls (1.6)

$$(EI)_{eff} = 0.4 E_m I_o \text{, for unreinforced walls} \tag{1.7}$$

where E_m represents the modulus of elasticity of the masonry, I_o represents the initial second moment of area of the wall cross-section about its centroidal axis before cracking, I_{cr} represents the second moment of area of the cracked section and e_k represents the kern eccentricity.

The total moment (once secondary moment is accounted for) and axial load applied to the wall are then further used in checking the compressive and moment resistance of the designed wall. As per the Standard (2014), unreinforced walls cannot be built to a slenderness ratio of 30 or greater, while the axial load on a reinforced wall cannot exceed (as per CSA S304-14 Clause 10.7.4.6.4):

$$P_f = 0.1 \phi_m f'_m A_e \tag{1.8}$$

where ϕ_m represents the resistance factor for masonry, f'_m represents the masonry compressive strength and A_e represents the wall's effective cross-sectional area.

1.3 Research Problem to Be Addressed by Thesis

Previous studies have investigated the claim that the Canadian Standard (2014) underestimates the capacity of slender masonry walls when walls are under eccentric axial load. Evidence that slender masonry wall capacities are significantly underestimated in CSA S304-14 (2014) was presented by Müller et al. (2017), upon studying results from many known testing programs in which slender masonry walls had been tested. The behaviour of the walls was compared to the expected wall capacities, as per CSA S304-14 (2014). It was demonstrated quantitatively that the design procedure for slender masonry walls in the Standard can significantly underestimate the strength of masonry walls for which slenderness must be considered, leading to an overly conservative design. The researchers claim that the reason for the overly conservative slender wall design procedures in CSA S304-14 is the inaccuracy in the magnification of the acting moment to account for the secondary moment (which is caused by axial load acting over the lateral deflection of the wall), leading to a large reduction of the wall's allowable load-bearing capacity. As the acting moment magnification depends on both the applied axial load and the critical axial load (itself a function of the wall's effective flexural stiffness and effective height), Müller et al. (2017) identify error in the estimation of effective flexural stiffness as well as the inaccurate prediction of fixity conditions as the two main sources of error in determining slender masonry wall capacity. The research suggested that the underestimation of slender masonry wall axial capacity is particularly large when axial loads are applied at low eccentricities, causing a relatively low initial primary moment. However, at higher axial load eccentricities, the design prescriptions in the Standard were believed to be much more accurate in predicting the behaviour of the wall.

Isfeld et al. (2019) compared the design of concrete block slender masonry walls in the Canadian Standard, CSA S304-14, (2014) to other national masonry design standards. In Figure 1.1 below, originally published by Isfeld et al. (2019), the relationship between the total reduction factor (relative to the wall's cross-sectional material capacity when loaded in pure compression) and a masonry wall's height to thickness ratio is shown. It can be observed that each design standard shown other than CSA S304-14 (2014) has a gradual drop in reduction factor as a wall's height to thickness ratio is increased, while in CSA S304-14 (2014) a sudden drop in the applied reduction factor can be observed at a height to thickness ratio of 30. As CSA S304-14 (2014) prescribes an allowable axial load reduction factor of 90% (of the original factored axial strength of the effective cross-section) when the slenderness ratio equals or exceeds 30, this steep drop is unreasonable (considering a wall with a slenderness ratio just under 30 would not have to have its allowable axial load limited to 10% of its original compressive strength). All other design standards shown have discretized the relationship shown in Figure 1.1.

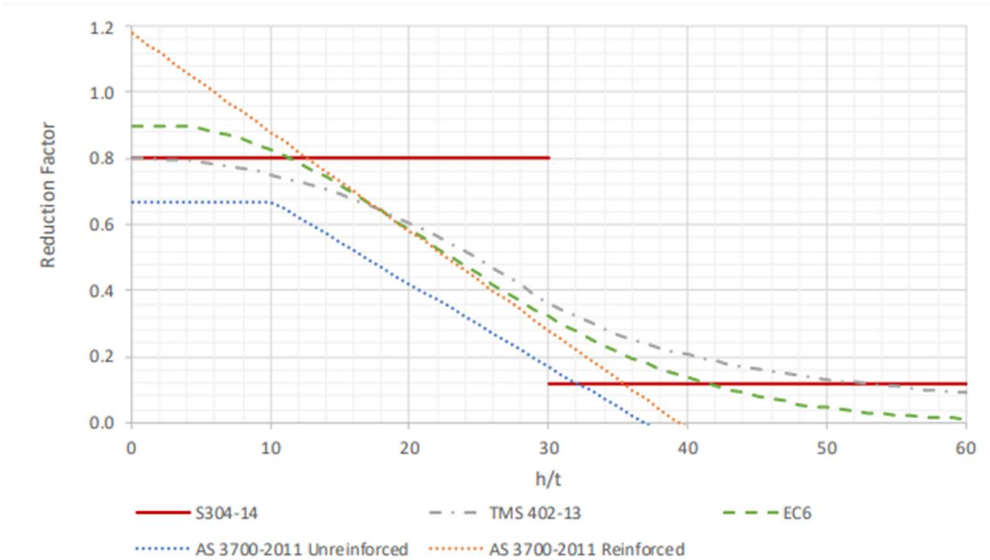

Figure 1.1 Height to Thickness Ratio vs. Reduction Factor in Different Design Standards, Taken from Isfeld et al. (2019)

In comparing the various design standards, the sudden drop in allowable axial strength prescribed only in CSA S304-14 raises concerns that at height to thickness (h/t) ratios over 30, walls are being overdesigned, while suggesting that walls with h/t ratios just under 30 may not be safe. The behaviour of slender masonry walls around an h/t ratio of 30 is of particular concern, as the Alberta Masonry Council (2020) observes that it may be indicating a common industry practice to design many walls to have a slenderness ratio just under 30 to avoid the required restrictive drop in allowable axial load. It was noted by the Alberta Masonry Council (2020) that concrete block walls are commonly used in the construction of school gymnasia, which according to Alberta Infrastructure requirements must have a clear height of 9.1 m (roughly 30ft) between the floor and underside of the roof framing. Using the common 190 mm block would force the slenderness ratio of a standard gymnasium wall to over 30. In these cases, common practice for design engineers is to use a thicker block to push the slenderness ratio to just below 30, suggesting that presumably many walls are being designed in this range (which, according to all the other national design standards shown in Figure 1.1 would make these walls unsafe). Building a thicker wall is also significantly less economical due to the additional material costs which are incurred. Dr. Hagel, of the Alberta Masonry Council (2020), also notes four schools constructed within an eight-month period in Edmonton for which concrete tilt-up walls were chosen over concrete block walls due to the lower construction cost of the tilt-up walls, according to the general contractor in charge of the projects. As per the Canadian Wood Council Tall Walls Workbook (2000), wood stud walls can be designed to up to a 10.7 m height in commercial structures without greatly limiting their load-bearing capacity. For comparison, a 10.7 m tall slender masonry wall (assuming pinned connections) built with standard concrete block would have a slenderness ratio of 56, meaning the allowable axial load would have been greatly reduced. Masonry walls of equivalent heights are not commonly being constructed. This is a very concerning trend for the masonry industry, as it was noted by the Canadian Masonry Council (2020) that in recent years the masonry industry has lost jobs both in Alberta and Ontario. Considering these developments, the aim of this thesis is to research the slender wall design provisions in the Canadian Standard (2014) in order to improve the safety and economic feasibility of slender masonry wall design and construction.

1.4 Thesis Outline

The previously mentioned research papers have identified inconsistencies and inaccuracies in the CSA S304-14 (2014) procedure for the design of slender masonry walls. Such findings are consistent with the experiences within the masonry industry with the design and construction of slender masonry walls. This thesis will aim to build on previous works dealing with the issue of slender masonry wall design in the Canadian Standard, further clarifying the sources of error present in the Standard and seeking to contribute to a theoretical foundation for a more refined slender masonry wall design procedure.

This thesis will focus on the accuracy of the determination of the effective stiffness as per the Standard and will propose a more accurate approach to estimating a wall's stiffness as it cracks under increasing moment. Ultimately, an alternative approach for categorization of walls as to whether they experience slenderness effects or not will be proposed based on the expected wall failure mode. Analysis was conducted using the findings of the Hatzinikolas et al. (1978a) testing program completed at the University of Alberta, for which a large number of full-scale slender concrete block walls were tested to failure. It is pertinent to observe that while the Canadian Standard applies to all masonry construction, the analysis in this thesis focuses primarily on walls constructed of standard concrete blocks. This is a limitation which must be understood for the findings of this thesis to be properly contextualized.

Chapter 2: Literature Review

2.1 Introduction

The purpose of this chapter is to contextualize the work carried out for this thesis as part of a larger body of work which had been developed from the study of slender masonry walls with a particular focus on understanding and defining the factors which influence their strength and behaviour. Relevant experimental programs will be described and the most relevant theoretical studies leading up to the work discussed in this thesis will be highlighted. These studies generally sought either to develop a deeper understanding of slender masonry wall behaviour or to identify inaccuracies in the slender wall procedure of the Canadian Standard for the Design of Masonry Structures, CSA S304-14, (2014) and to contribute to the development of more accurate design guidelines.

2.2 For Reference: Overview of the Canadian Standard for the Design of Masonry Structures, CSA S304-14, (2014) As It Relates to the Design of Slender Masonry Walls

The Canadian Standard for the Design of Masonry Structures, CSA S304-14, (2014) distinguishes between masonry walls based on their slenderness ratio and outlines a robust design procedure for each category of wall. This chapter relates most closely to the work which was carried out as part of the research described in this thesis and many of these equations will be referenced throughout this chapter. The equations are noted as they appear in the Canadian Standard, though in the analysis summarized throughout this thesis resistance factors are not applied unless explicitly stated otherwise.

Slenderness is deemed a necessary consideration (both for reinforced and unreinforced walls) when:

$\frac{kh}{t} \geq \left(10 - 3.5\left(\frac{e_1}{e_2}\right)\right)$ Clauses 7.7.5.1/10.7.3.3.1 – (2.1)

where k represents the effective length factor for a compression member, h represents the wall height, t represents wall thickness, and e_1 and e_2 represent top and bottom axial load eccentricity respectively.

As per Clause 7.7.5.2, when designing unreinforced walls, the effective height to thickness ratio ($\frac{\mathrm{kh}}{\mathrm{t}}$) must never exceed a value of 30. When designing reinforced walls, as per Clause 10.7.4.6.1, when $\frac{\mathrm{kh}}{\mathrm{t}} > 30$, the wall must be designed with consideration for slenderness, with additional provisions (CSA S304-14, Clause 10.7.4.6). Most importantly, this provision limits the total factored axial load:

$P_f \leq 0.1\phi_m f'_m A_e$ Clause 10.7.4.6.4 – (2.2)

where $\mathrm{P_f}$ represents the factored axial load, ϕ_{m} represents the resistance factor for masonry, $\mathrm{f'_m}$ represents the compressive strength of masonry normal to bed joint at 28 days and $\mathrm{A_e}$ represents the effective cross-sectional area of masonry.

When the effect of slenderness must be considered in the design of masonry walls, the secondary moment effect must be accounted for in the total design moment. This can be achieved either by using the load displacement (P-δ) method (CSA S304-14, Clause 7.7.6.2/10.7.4.2) or the moment magnifier method (CSA S304-14, Clauses 7.7.6.3/10.7.4.3).

The load displacement method is defined as follows:

$M_{ftot} = M_{fp} + P_f\delta_f$ Clauses 7.7.6.2.1/10.7.4.2.1- (2.3) where M_{ftot} represents the total factored moment (including secondary moments), M_{fp} represents the factored primary moment at the section due to the end factored moments and lateral loads, P_f represents the factored axial load and δ_f represents the lateral deflection of walls or columns at the critical section under factored lateral and axial loads (including the effect of secondary moments).

The lateral deflection, δ_f, is calculated using the rigidity coefficient:

$$\phi_{er}(EI)_{eff}/(1+0.5\beta_d) \qquad \text{Clauses 7.7.6.2.2/10.7.4.2.2 – (2.4)}$$

where ϕ_{er} is taken as 0.75 (ϕ_e is taken as 0.65 for unreinforced walls), $(EI)_{eff}$ represents the effective stiffness of the wall and β_d represents the ratio of factored dead moment to total factored moment.

The moment magnifier method is:

$$M_{ftot} = M_{fp}\frac{C_m}{1-\frac{P_f}{P_{cr}}} \geq M_{fp} \qquad \text{Clauses 7.7.6.3/10.7.4.3 - (2.5)}$$

where M_{fp} represents the maximum factored primary moment of the member due to the end factored moments and lateral loads.

$C_m = 0.6 + 0.4\,M_1/M_2 \geq 0.4$ where $M_2 \geq M_1$; with both M_1 & M_2 representing end moments and the C_m factor relating the actual moment diagram to an equivalent uniform moment diagram.

$P_{cr} = \pi^2\phi_{er}(EI)_{eff}/[(1+0.5\beta_d)(kh)^2]$, with P_{cr} representing the critical axial compressive load, k representing the effective height factor, ϕ_{er} representing the resistance factor for member stiffness used in the determination of slenderness effects on the capacity of reinforced masonry (ϕ_e is used for unreinforced masonry) and β_d representing the total factored dead load moment to total factored moment ratio.

The effective stiffness, EI_{eff}, for reinforced walls is calculated using the following equation (CSA S304-14, Clause 10.7.4.4):

$$(EI)_{eff} = E_m[0.25I_o - (0.25I_o - I_{cr})(\frac{e-e_k}{2e_k})] \leq 0.25E_mI_o \text{ but} \geq E_mI_{cr} \qquad \text{Cl. 10.7.4.4 - (2.6)}$$

where $\mathrm{E_m}$ represents the modulus of elasticity of masonry, $\mathrm{I_o}$ represents the second moment of area of the effective cross-sectional area about its centroidal axis, $\mathrm{I_{cr}}$ represents second moment of area of the compression zone and the transformed area of the tension steel about the centroidal axis of the cracked section when subjected to a moment larger than cracking moment, e represents the virtual eccentricity and $\mathrm{e_k}$ represents kern eccentricity value for the effective cross-sectional area.

The effective stiffness, EI_{eff}, for unreinforced walls is calculated using the following equation (CSA S304-14, Clause 7.7.6.4):

$$(EI)_{eff} = 0.4E_mI_o \qquad \text{Clause 7.7.6.4 – (2.7)}$$

where $\mathrm{E_m}$ represents the modulus of elasticity of masonry and $\mathrm{I_o}$ represents the second moment of area of the effective cross-sectional area about its centroidal axis.

The total moment (which includes the secondary moment) together with the applied axial load would then be used to design the wall cross-section, typically by comparing the applied moment and axial load on the wall to the P-M interaction curve.

2.3 Work Directly Prompting This Thesis

The analysis published in this thesis was built directly on the works presented below, as will become apparent in subsequent chapters.

2.3.1 Müller et al. (2017): Review and Analysis of Capacity of Slender Concrete Masonry Walls

The research conducted by Müller et al. (2017), presented in "Review and Analysis of Capacity of Slender Concrete Masonry Walls", has served as the impetus for the research which is being presented in this thesis. It was Müller et al. (2017) who first quantitatively demonstrated that in the Canadian Standard, CSA S304-14 (2014), the capacity of slender masonry walls is being underestimated. The authors noted that this led to a significant overdesign of slender walls in practice. Müller et al. (2017) identified that the capacity of a slender masonry wall loaded axially is mainly affected by the wall's slenderness ratio, the applied axial load eccentricity, the deflected shape of the wall (which depends on the end conditions at the top and bottom of the wall) as well as by the flexural stiffness of the wall. Müller et al. (2017) analyzed nine testing programs in which slender walls were loaded axially and at times laterally and tested to failure; they produced tables comparing the experimental failure loads of the walls to predicted failure loads as per the Canadian Standard. The underestimation in design capacity in the slender wall design provisions in the Standard is quantitatively demonstrated and the inaccuracy is shown to be more significant as walls are taller and axial load eccentricities are smaller. Additionally, the capacity of slender walls is predicted more inaccurately by the Standard when the walls are loaded with greater axial load (relative to the lateral load). The main reason for the inaccuracy in design was found to be the effective stiffness calculation method in the Standard (see Equations 2.6 and 2.7 above). The effective stiffness was found to be particularly conservative at low axial load eccentricities and it was noted that further research is required to understand the effective stiffness of a slender wall better as it is loaded under site conditions. A recommendation was made that a future equation for the effective stiffness, EI_{eff}, should consider the slenderness ratio (h/t) and the relative eccentricity of a wall (e/t). It is also noted that the neglect of the rotational stiffness consideration at the bottom of the wall also contributes to the conservative design as per the Standard.

2.3.2 Isfeld et al. (2019): Finite Element Analysis of Hollow Concrete Block Masonry Walls

Isfeld et al. (2019) modelled ungrouted and unreinforced concrete block walls at varying slenderness ratios and eccentricities using a micro-modelling approach within finite element modelling (the testing program based on which these models are calibrated is described in section 2.4.9, Isfeld et al. (2020)). The slenderness ratios of modelled walls spanned from height to thickness ratios of 5 to 60 and the applied axial load eccentricities ranged from 0 to t/2 (half the wall thickness). The end conditions of the walls used in the models were both fixed-fixed and pinned-fixed, with both fixity conditions thought to be more accurate than pinned-pinned conditions when it comes to the reality of an actual wall built on a construction site. The maximum axial loads and the lateral displacements of the walls were reported. The findings shown by Isfeld et al. (2019) give strong indications about the failure mode of each wall (at varying axial load eccentricities). Isfeld et al. (2019) concluded that the walls were failing at higher loads than had been conservatively considered by the Canadian Standard, CSA S304-14 (2014). In particular, the Standard limits the design capacity of slender walls above a slenderness ratio of 30 to 10% of the wall's compressive strength (see Equation 2.2 above), which Isfeld et al. (2019) found to be overly conservative based on the results presented (this is exemplified in Figure 1.1 in the "Thesis Overview" chapter). As Isfeld et al. (2019) indicated the nature of the failures predicted by the models for each wall, it was also noted that walls loaded at low axial low eccentricities (even among the most slender walls modelled) were expected to fail by experiencing material failure (specifically, the paper notes if a wall is expected to fail with bed joints open, closed, or partially open). This finding will be discussed further in this thesis, where it will be suggested that many slender walls which are loaded at low axial load eccentricity are being significantly overdesigned because their failure mode is being incorrectly predicted in the Standard by the secondary moment effects being overemphasized in the design of such walls.

2.3.3 Bogoslavov & Shrive (2020): The Influence of Effective Flexural Stiffness on Slender Masonry Wall Capacity

Bogoslavov & Shrive (2020) is entirely contained within this thesis, in particular the work reported in this publication is contained within most of the “Methodology and Results” chapter. As part of this work, the degree to which the effective stiffness term, EI_{eff}, is conservatively calculated in the Canadian Standard is assessed. The causes of this inaccuracy are discussed and a different approach to the design procedure is suggested, whereby the failure mode of slender walls is first predicted based on the axial load eccentricity and height to thickness ratio.

2.3.4 Ahmed et al. (2021): Examining the Mode of Failure of Slender Concrete Block Walls

Ahmed et al. (2021) is explored in depth in the “Analysis and Discussion” chapter of this thesis, as the author of this thesis was one of the co-authors of the paper. It builds on the work of Isfeld et al. (2019) and Bogoslavov and Shrive (2020), with the latter paper already having published much of the work discussed in this thesis relating to the assessed inaccuracy of the EI_{eff} calculation procedure in the Canadian Standard. To briefly summarize the work by Ahmed et al. (2021), the purpose of the paper was to assess the loading conditions required for different failure modes to occur. The research built on the work of Isfeld et al. (2019) cited above, where it was determined that slender walls loaded at low axial load eccentricities typically experienced material failure, rather than out-of-plane failure, as would be expected of a slender wall. This is a particularly telling fact when viewed in conjunction with a conclusion drawn by Müller et al. (2017), that the Canadian Standard is particularly conservative in the design of slender walls loaded at a low axial load eccentricity. In order to assess whether unreinforced concrete block slender walls which are lightly loaded laterally (at roughly the magnitude of a typical wind design load) and at a low axial load eccentricity will still experience material failure, walls of varying slenderness ratios (h/t = 10, 20, 30, 40) were modelled by Ahmed et al. (2021). The walls were modelled to be loaded axially at low load eccentricities (e = 0, t/10, t/6) and laterally at a typical wind design load as per the National Building Code of Canada (2015); their failure mode was assessed based on the degree to which the bed joints were open or closed at failure. It was concluded that the additional lateral load of this magnitude did not lead to the slender wall models showing signs of flexural failure when loaded at low axial load eccentricities.

2.4 Experimental Testing Programs and Studies Based on Computer Analysis

The following studies are presented to give the reader a general idea of the chronology and development of the knowledge base surrounding slender masonry walls. The testing program by Hatzinikolas et al. (1978a) has been heavily referenced in particular for the writing of this thesis, as ultimately the results of that testing program were used in the analysis presented in this thesis.

2.4.1 Yokel et al. (1970): Compressive Strength of Slender Concrete Masonry Walls, Yokel et al. (1971): Strength of Masonry Walls Under Compressive and Transverse Loads

Yokel et al. (1970) tested 60 slender reinforced and unreinforced concrete masonry walls of varying thickness and slenderness which were loaded at varying axial load eccentricities. At the time, there were few experimental data available, and the slenderness was considered in design by using a stress correction factor or empirical equation. Yokel et al. (1970) proposed the use of the moment magnifier method (a modern approach of this method is shown above, see Equation 2.5) in the design procedure for slender masonry walls in order to account better for the secondary moment effects experienced by slender walls. As Yokel et al. (1970) report, a significant number of walls tested experienced local failure close to one of the wall supports. It is possible that this is caused by an issue in the testing procedure, such as the vertical load not being adequately spread onto the width of the wall. As such, these results were not used in this thesis for analysis.

Yokel et al. (1971) tested a further 90 walls built of varying masonry units and mortars. The walls were tested to failure with the application of a lateral load, a compressive axial load or both. While it was deemed that the wall strengths could be conservatively predicted, it was noted that further research was required to better predict the change in a wall's slenderness as it is loaded. In particular, it is stated that the effect of cracking on the stiffness and the change in the value of the elastic modulus should be further studied.

2.4.2 Hatzinikolas et al. (1978a): Concrete Masonry Walls, Hatzinikolas et al. (1978b): Experimental Data for Concrete Masonry Walls

As part of their experimental program, Hatzinikolas et al. (1978a) tested 68 full scale concrete block masonry walls to failure. The walls of differing slenderness ratios, reinforcement and axial load eccentricity were loaded axially to failure. Due to the large number of walls tested, many of the tested walls varied by only one parameter, thus making it possible to examine these parameters with accuracy. For example, groups of walls were built to the same slenderness and reinforcement ratio, but then loaded at differing axial load eccentricities. The results of these tests were presented as part of an extensive testing program report, with the strain, vertical deflection and lateral deflection all graphed against the applied axial loads on the walls. The results report, also published by Hatzinikolas et al. (1978b), is named "Experimental Data for Concrete Masonry Walls."

From the analysis conducted by Hatzinikolas et al. (1978a) many conclusions are drawn about the behaviour and design of concrete block walls. It was concluded that walls loaded in double curvature are significantly stronger than walls loaded in single curvature. The moment magnifier method (see Equation 2.5 above) was noted as adequate for the consideration of the effect of slenderness on wall capacity, though it is recommended that further research be carried out to study wall stiffness (EI_{eff}) further as the wall is being loaded. Uncertainty in the modulus of elasticity calculation was also expressed, with the suggestion being that only the experimental evaluation is a very accurate method for determining the modulus of elasticity. It was further observed that walls which were loaded at low axial load eccentricity tended to experience material failure, rather than flexural failure. These results are further referred to in the “Methodology and Results” chapter of this thesis.

2.4.3 Ojinaga and Turkstra (1980): The Design of Plain Masonry Walls

In this work, Ojinaga and Turkstra assessed the design of plain masonry walls by critically examining relevant academic literature. A design approach is outlined for unreinforced masonry walls. The moment-magnifier theory is analyzed (see Equation 2.5 above for its current adapted form) and its applicability to masonry is discussed. It is noted that a major weakness of the theory is that to calculate the critical buckling load the original stiffness (EI) is considered (in the current Canadian Standard, as shown above in Equations 2.6 & 2.7, this issue has been addressed with equations for effective stiffness). Thus, out of the need to predict the effect of cracking of the masonry units, two equations are proposed for the approximation of effective stiffness of unreinforced masonry walls:

1) $I_{eff} = (I_{END1} + I_{END2})/4$, for walls experiencing single curvature bending (2.8)
2) $I_{eff} = \min\{(I_{END1} + I)/4 , (I_{END2} + I)/4\}$, for double curvature bending (2.9)

where I_{eff} represents the effective second moment of area, I_{END1} and I_{END2} represent the second moments of area at either end of the wall (typically cracked sections) and I represents the uncracked section second moment of area.

For the case of the wall experiencing single curvature bending (the ratio of top and bottom eccentricities is positive), it is known that a hinge forms at about the midspan of the wall as the wall cracks through its thickness and so the second moment of area at this location approaches a value of 0 at failure. As such, the equation referring to single curvature bending above represents the average of the top and bottom end values and the midspan value. For walls experiencing double curvature bending, a section of the wall is expected to remain uncracked and thus it is represented in the double curvature bending equation above by the uncracked section second moment of area being considered in the equation. This method was ultimately not included in the Canadian Standard, as alternative equations are currently used to calculate a wall's effective stiffness (see Equations 2.6 & 2.7 above).

2.4.4 Ojinaga and Turkstra (1982): Design of Reinforced Masonry Walls and Columns for Gravity Loads

In their 1982 journal paper, Ojinaga and Turkstra (1982) assess the design of reinforced masonry walls subjected to vertical axial load of varying eccentricities. It is noted that the current theory for axially loaded walls at an eccentricity is quite conservative. A particular focus is placed on a method which considers the effect of slenderness. Two equations from their previous work, Ojinaga and Turkstra (1980), are adapted to reinforced masonry walls. The two following equations are presented:

1) $I_{eff} = (I_{END1} + 2I_{cr} + I_{END2})/4$, for walls experiencing single curvature bending (2.10)
2) $I_{eff} = \min\{(I_{END1} + 2I_{cr} + I)/4\ ,\ (I_{END2} + 2I_{cr} + I)/4\}$, for double curvature bending (2.11)

where I_{eff} represents the effective second moment of area, I_{END1} & I_{END2} represent the moments of inertia at either end of the wall (typically cracked sections), I represents the uncracked section second moment of area and I_{cr} represents the cracked second moment of area.

The equations presented above serve to approximate a second moment of area (and thus an effective stiffness) value to reflect a reduced cross-sectional area due to cracking as a slender wall is loaded. To achieve this, an average second moment of area is arrived at by taking a mean second moment of area value across four locations along a wall's height. In the case of a wall experiencing single curvature bending, the two end second moments of area are considered as well as two times a cracked second moment of area (second moment of area when the section is experiencing pure moment). Meanwhile, for walls which are experiencing double curvature bending, hinges can form at two locations, which is why two cracked second moments of area are averaged together with a second moment of area at the end of the wall (which represents a reduction in the cross-sectional area) as well as with a second moment of area taken at a section of the wall which is expected to remain uncracked.

2.4.5 ACI-SEASC Task Committee on Slender Walls (1982): Test Report on Slender Walls

The American Concrete Institute and the Structural Engineers Association of Southern California Task Committee tested 30 slender walls made up of the following varying materials: tilt-up concrete, concrete blocks, clay bricks and clay blocks. All walls were loaded laterally (to simulate wind or seismic load) and vertically at an eccentricity (to simulate a vertical roof load), though the axial loads were limited to 10% of the compressive strength of the wall. A detailed analysis was conducted, and the behaviour of the varying materials was compared. As most of the moment resisted by the walls was caused by the lateral load, the report determined that the eccentric moment from the applied axial load was not largely significant. It was stated that about 20% of the moment at the yield of reinforcement was a product of a secondary moment effect. Several design recommendations were suggested. One particular suggestion was that deflection control must be applied in order to limit the effects of the secondary moment and the accompanying reduction in stiffness, rather than limiting height to thickness ratio directly.

2.4.6 Suwalski (1986): Capacity of Eccentrically Loaded Slender Concrete Block Walls

Suwalski (1986) tested to failure 14 slender concrete block walls (six were unreinforced, eight were reinforced). Axial vertical loads were applied at varying eccentricities to 12 of the walls while two were loaded in pure bending. Similar to the results reported by Hatzinikolas et al. (1978b), slender walls loaded at an eccentricity of one sixth of the wall thickness or less experienced a material compressive failure, rather than a flexural failure, as would be expected of a slender wall. It is concluded that the effect of slenderness becomes significant above a certain increase in eccentricity and slenderness ratio (in the case of this study above a height to thickness ratio of 25). This observation is consistent with later research conducted by Isfeld et al. (2019) and Ahmed et al. (2021), who observed and then further studied the phenomenon of slender concrete block walls failing in compression rather than in flexure when loaded at low enough axial load eccentricities. Suwalski (1986) also further comments on the Canadian Masonry Standard provisions which were in place at the time and observes that slender walls being designed at large axial load eccentricities are likely not being designed conservatively enough, while walls designed at low axial load eccentricities are likely being overdesigned.

2.4.7 Mohsin & Elwi (2003): Effect of Implied Fixity at Masonry Block Wall-Support Interface on Stability of Load Bearing Walls

Mohsin and Elwi (2003) sought to determine the effect of support rotational stiffness (fixity condition) on the buckling capacity of masonry block walls. Two groups of slender walls were loaded axially to failure (built to height to thickness ratios of 28.6 and 33.9 respectively) while the rotational stiffness at the base of the walls was varied between specimens. The effect of the stiffness at the bottom wall support was noted as significant, as that stiffness influenced the wall's deformed shape significantly. The effect of the support stiffness on the axial capacity of a slender wall was found to be greater at a lower height to thickness ratio. It was also demonstrated that a wall's support stiffness also influences the actual effective flexural stiffness, EI_{eff}, of a wall as it is being loaded, with an increase in a wall's support rotational stiffness leading to a higher effective stiffness. Mohsin & Elwi also noted that the calculation of a masonry wall's effective stiffness in the Canadian Standard is overly conservative. While this thesis does not examine in greater depth the effect of fixity conditions on slender masonry wall design, the research conducted by Mohsin & Elwi (2003) remains relevant and necessary for a deeper understanding of slender masonry wall behaviour. Müller et al. (2017) also noted the consideration of fixity in the design of slender masonry walls as a potential area of inaccuracy which contributes to the conservatism in the design.

2.4.8 Liu & Hu (2007): Experimental Study of Reinforced Masonry Walls Subjected to Combined Axial Load and Out-of-Plane Bending, Liu & Dawe (2003): Analytical Modeling of Masonry Load-Bearing Walls

Liu and Hu (2007) tested to failure 12 reinforced masonry walls all at a slenderness ratio of 17.1 with pinned-pinned support conditions, at varying axial load eccentricities. The effective flexural stiffness, EI_{eff}, was recorded as the walls were loaded and EI_{eff} was varied as walls were loaded at different eccentricities and top and bottom eccentricity ratios. As the comparison was made between the recorded EI_{eff} values and the calculated EI_{eff} values (using the Canadian Masonry Standard, see Equations 2.6 & 2.7 above), it was observed that the Canadian Standard underestimates EI_{eff}, in particular when material (crushing) failure dominates. As material failure is more likely to occur as walls are loaded at a lower axial load eccentricity, this would mean that walls loaded at low axial load eccentricities are being particularly overdesigned. This same claim was further reinforced by both Müller et al. (2017) and Isfeld et al. (2019), as both demonstrated this quantitatively. Isfeld et al. (2019) correlated a wall's height to thickness ratio and axial load eccentricity to its failure mode directly. In this thesis the idea of discretizing slender masonry wall design procedures based on the predicted failure mode is explored further.

Liu and Hu (2007) report on equations originally proposed by Liu and Dawe (2003) to better estimate the effective stiffness, EI_{eff}, of reinforced slender masonry walls as they are loaded to failure. The equations were originally developed based on over 500 computer-ran models:

1) $EI_{eff}/EI_o = 0.7$, when $0 \le e/t \le 0.1$ (2.12)
2) $EI_{eff}/EI_o = 1 - [2.375 - (0.0175h/t)](e/t)$, when $0.1 \le e/t \le 0.4$ (2.13)

3) $EI_{eff}/EI_o = [0.05 + (0.007h/t)]$, when $e/t > 0.4$ (2.14)

Interestingly, in cases where the axial load eccentricity of the applied vertical load is greater than 0.4 times the wall thickness, the above equation predicts that the effective stiffness term is greater as a wall of higher height to thickness ratio is loaded. Liu and Hu (2007) did show by comparing their experimental results with the Canadian Standard that these proposed equations do allow for a more accurate prediction of EI_{eff} for walls loaded at a lower axial load eccentricity, as compared to the Standard.

2.4.9 Isfeld et al. (2018): Analysis of Safety of Slender Concrete Masonry Walls in Relation to CSA S304-14, Isfeld et al. (2020): Testing and Finite Element Modelling of Concrete Block Masonry Walls Under Axial and Out-of-Plane Loading

Isfeld et al. (2018) conduct an overview of the design procedure for slender masonry walls, with a summary of the pertinent theory with respect to the design equations presented in the paper. Previous wall testing programs are summarized and it is demonstrated that the results reported by the various testing programs generally indicate that the design provisions for slender wall design in CSA S304-14 (2014) underestimate wall strength, in particular when high vertical loads are applied at a low axial load eccentricity. Three concrete block walls were constructed by Isfeld et al. (2018) and tested to failure. It is noted that the testing and subsequent analysis indicate that the displaced wall profile recorded as the walls are being loaded resembles the profile of a wall with fixed-pinned end conditions when the bottom support is not forced to act as a pinned connection. However, it is a typical conservative assumption to design slender walls for pinned connections at the top and the bottom of the wall. As such, it is concluded that using an effective height factor (k) of 1 (corresponding to pinned connections and the top and the bottom of the wall) contributes to the overdesign of slender walls in CSA S304-14.

The issue of the bottom base support is further explored by Isfeld et al. (2020). As part of this analysis, three concrete block walls were tested to failure (both axial and out-of-plane loads were applied) and the results were used to calibrate a set of finite element models, for which a micro-modelling approach was used. It was determined that the actual behaviour of the wall at its base was somewhere between being pinned and fully fixed. When a wall was only loaded vertically, about 90% of the wall base remained in contact with the supporting steel plate on which it was sitting, while this contact area was a little smaller when a wall is loaded out-of-plane. Nevertheless, it was concluded that assuming a pinned connection at the base of the wall is overly conservative, in particular when construction site conditions are taken into account.

2.5 Summary

The aim of this chapter was to provide the reader with a general overview of the literature relating to slender masonry wall design and to contextualize this thesis within a greater body of work. The reader is now aware of the paucity of research on slender concrete block walls, whether they be plain, partially grouted (possibly reinforced) or fully grouted and reinforced. Earlier work concentrated on brickwork and is not reviewed here although it should be recognized that the definition of slenderness as the height to thickness ratio is a consequence of that earlier work: brickwork is deemed solid, so there is a constant ratio between radius of gyration and thickness. In particular, this review of the literature related to concrete blockwork should help the reader draw conclusions regarding the relevance of the work presented in this thesis.

Chapter 3: Methodology and Results

3.1 Introduction

In this chapter the research methodology of the analysis is laid out. Due to the linear nature of this research project, with the next step in the analysis constantly building on previous results, it was necessary to include the results obtained from each step in the analysis in this chapter. Throughout this chapter, the effective stiffness term is explored. The degree of error in the calculation of the term as per the Canadian Standard (CSA S304-14 (2014)) is first established. The Hatzinikolas et al. (1978a) testing program is further scrutinized and possible sources of error are quantitatively examined. The work described in this section leads to a more accurate prediction of the actual stiffness of slender concrete block walls as they are being axial loaded and the presentation of critical findings, aimed at better informing a future development of a more accurate effective stiffness equation.

3.2 Assessing Error in Effective Flexural Stiffness Term as per CSA S304-14 (2014)

In “Review and Analysis of Capacity of Slender Concrete Masonry Walls”, Muller et al. (2017) quantitatively demonstrated that the CSA S304-14 (2014) design procedure for slender masonry walls was overly conservative. The study identified the effective stiffness (EI_{eff}) term as a significant source of error and thus substantially contributing to the underestimation of slender masonry wall capacity in the Standard. It was recommended in the paper that the effective stiffness term calculation be further investigated and upon further research a more accurate equation be developed to estimate the loss of stiffness as the walls crack.

The paper by Muller et al. (2017) therefore served as an impetus for the analysis conducted as a part of this thesis. The first step in this analysis was to investigate further the claim that the effective stiffness term was the primary source of error in the design of slender masonry walls. To do this, the degree of error in the calculation of the effective stiffness term for a variety of wall designs and loading configurations had to be determined. Using the deflection equation (Equation 3.1 below), itself derived using the moment area theorems, the lateral deflection of slender walls could be calculated and compared to the actual lateral deflection of slender walls which have themselves been tested. Such an analysis allows for a relatively accurate examination of the effective stiffness term, as the calculated deflection is directly dependent on the stiffness of the member. The effect of other potential sources of error can be minimized due to the previously established accuracy of the deflection equation (Equation 3.1) and the load displacement and moment magnifier methods as shown in Equation 1.2 and Equation 1.5 (see "Thesis Overview" chapter), respectively (both of which produce relatively consistent results between each other, as was noted by Müller et al. in 2017).

The following equation is used to calculate the lateral deflection of masonry walls (from CSA S304-04 Commentary Section 7.5.2):

$$\delta_f = \frac{M_{ftot}(kh)^2}{8EI} \tag{3.1}$$

where $\mathrm{M_{ftot}}$ represents the total moment (including secondary moments), kh represents the wall effective height (accounting for end conditions). EI, the stiffness, is calculated using the rigidity coefficient, as per clauses 7.7.6.2.2/10.7.4.2.2 (with β_d taken as 1, and the effective stiffness, $(\mathrm{EI})_\mathrm{eff}$, calculated as per Equations 1.6 or 1.7 in the "Thesis Overview" chapter): EI = $(EI)_{eff}/(1 + 0.5\beta_d)$.

The calculated and the measured lateral deflections were compared using data from the extensive testing program conducted by Hatzinikolas et al. (1978a). These data were presented in Structures Report No. 70 and Structural Engineering Report No. 71, both published at the University of Alberta in 1978. The Hatznikolas et al. (1978a) testing program was used due to its extensive scope and the detailed results which were published. As part of the testing program, sixty-eight full-scale concrete block walls were tested to failure, most of which are categorized as slender by the Canadian Standard. The walls, which varied in reinforcing, slenderness ratio (h/t) and effective cross-sectional area were vertically loaded at varying axial load eccentricities. The data were reported in detail, including lateral deflections, strains and vertical deformation of the slender walls as they were incrementally loaded.

The lateral deflections of the slender walls which were loaded to single-curvature failure as part of the Hatzinikolas et al. (1978a) testing program are recorded in Table 3.1 below (typically the greatest lateral deflection occurred around the midspan of each wall). For these walls, failure loads and loading conditions, the lateral deflection is calculated using the procedure in the Canadian Standard and the ratio of the calculated to the test deflection is shown in the last column of Table 3.1 below. In addition, wall slenderness ratio, vertical reinforcement, axial load eccentricity and failure load are reported in the table.

Table 3.1 Hatzinikolas et al. (1978b) Recorded Test Lateral Deflection vs. Calculated Lateral Deflection Using CSA S304-14 (2014)

Wall Name	Slenderness Ratio (m/m)	Vert. Reinf. (Imp.)	Eccentricity (mm)	Failure Load (kN)	Recorded Test Deflection (mm)	Calculated Deflection (mm)	**Calculated (CSA S304-14) to Test Deflection Ratio**
A1	13.8	Plain	19.4*	1246	1.3	25.4	**19.5**
A2	13.8	Plain	32.3	708	7.0	16.5	**2.4**
A3	13.8	Plain	64.5	357	10.0	13.8	**1.4**
A4	13.8	Plain	19.4*	1068	1.0	18.9	**18.9**
A5	13.8	Plain	76.2	116	8.0	4.8	**0.6**
B1	13.8	3#9	19.4*	1868	4.0	655.7	**163.9**
B2	13.8	3#9	32.3	1423	10.2	110.5	**10.9**
B3	13.8	3#9	64.5	622	26.7	37.7	**1.4**
B4	13.8	3#9	76.2	689	26.7	52.0	**2.0**
B5	13.8	3#9	88.9	511	19.1	39.3	**2.1**
C1	15.9	3#9	19.4*	890	1.0	37.3	**37.3**
C2	15.9	3#9	19.4*	1601	1.0	26.2	**26.2**
C3	15.9	3#9	32.3	1110	16.5	127.1	**7.7**
C4	15.9	3#9	64.5	556	25.6	49.1	**1.9**
C5	15.9	3#9	76.2	545	42.0	56.1	**1.3**
C6	15.9	3#9	88.9	400	40.6	41.5	**1.0**
D1	18.0	3#9	19.4*	1068	2.5	364.7	**145.9**
D2	18.0	3#9	19.4*	1868	3.3	39.1	**11.9**
D3	18.0	3#9	32.3	890	24.0	143.0	**6.0**
D4	18.0	3#9	64.5	484	40.6	59.0	**1.5**
D5	18.0	3#9	76.2	420	48.3	55.1	**1.1**
D6	18.0	3#9	88.9	369	53.3	52.7	**1.0**
H1	18.0	3#6	19.4*	1868	0.1	54.7	**1215.9**
H2	18.0	3#6	32.3	1154	15.0	56.5	**3.8**
H3	18.0	3#6	64.5	384	34.3	157.5	**4.6**
H4	18.0	3#6	76.2	290	43.2	134.1	**3.1**
H5	18.0	3#6	88.9	249	57.0	181.2	**3.2**

I1	18.0	3#3	19.4*	1423	0.1	41.7	**1042.2**
I2	18.0	3#3	32.3	965	16.5	47.2	**2.9**
I3	18.0	3#3	64.5	240	3.0	82.2	**27.4**
I4	18.0	3#3	76.2	146	4.0	67.8	**16.9**
I5	18.0	3#3	88.9	108	9.0	110.7	**12.3**
L1	24.3	3#9	19.4*	1868	15.0	71.3	**4.8**
L2	24.3	3#9	32.3	667	18.0	42.6	**2.4**
L3	24.3	3#9	64.5	400	76.2	142.7	**1.9**
L4	24.3	3#9	76.2	356	79.0	124.9	**1.6**
L5	24.3	3#9	88.9	326	96.0	120.2	**1.3**
M1	24.3	Plain	19.4*	623	5.0	95.8	**19.2**
M2	24.3	Plain	32.3	534	25.0	87.1	**3.5**

*In this case axial load was applied concentrically, but as per CSA S304-14 (2014) a minimum eccentricity of 19.4 mm (0.1t) is assumed for the calculation. Haztinikolas et al. (1978a) used blocks with a 194 mm thickness (the old nominal 8 inch blocks (actual width 7⅝ inches)), - such blocks are not commonly used in Canada today.

The ratios of calculated to test lateral deflection, as shown in the last column of Table 3.1, generally exceed the ratio of 1, which is indicative of a trend of overestimation in the lateral deflections calculated based on the procedure in the Canadian Standard. As the lateral deflection is directly dependent on the wall stiffness (as per Equation 3.1), it can be concluded that the effective stiffness term is being generally underestimated. The procedure in the Standard appears to be particularly underestimating the effective stiffness term when a slender wall is not experiencing significant flexure. In the cases of the experiments where the effective stiffness was particularly underestimated the walls were loaded at a low axial load eccentricity. In some instances (i.e. Walls B1, D1, H1, I1, etc.) the calculated to recorded deflection ratios are absurdly high because the walls themselves were loaded concentrically, whereas for the design of slender walls the Standard mandates that a minimum axial load eccentricity of one tenth of the thickness (t/10) is used in order to account for inaccuracy in construction. Aside from this discrepancy, it is evident that the effective stiffness equation in the Standard overestimates the degree to which slender masonry walls loaded at low axial load eccentricity will crack and therefore underestimates the effective stiffness value. For walls loaded at higher axial load eccentricities the ratio of the calculated to the measured deflection was found to be relatively low and, in some cases, approaching a value of 1.0 (i.e. in the cases of Wall Series C, D & L), meaning that the effective stiffness term calculation in the Standard is quite accurate in such instances.

Based on the evidence in Table 3.1, it is clear that the effective stiffness equation in the Standard does not adequately consider the wall's axial load eccentricity, as the error in the effective stiffness calculation typically increases with lower axial load eccentricities, while the degree of the error is not significantly affected by walls' slenderness ratios. A future design procedure in the Standard will therefore need to consider the axial load eccentricity in the effective stiffness equation more accurately.

3.3 Exploring High Error in Effective Stiffness Term at Low Axial Load Eccentricity

While in Section 3.2 it was established that the effective stiffness term was generally being underestimated, the reasons for the inaccuracy of the Standard EI_{eff} equation had to be better understood. It was necessary to assess the potential contribution to the inaccuracy of the following variables: the effect of a lack of precision in the testing procedure when applying the axial load at a particular eccentricity and the conservative provision of taking a minimum axial load eccentricity of 0.1 of the wall thickness.

3.3.1 Assessing Potential Error Due to Inaccuracy in Reported Axial Load Eccentricity

In seeking to understand better the experimental limitations of the Hatzinikolas et al. (1978a) testing program used in assessing the effective stiffness of slender concrete block walls as they are loaded eccentrically, it was relevant to assess the sensitivity of the reported results to common sources of error in a structures lab environment. While many qualitative assessments of the testing program were discussed in the previous “Literature Review” chapter, here a more quantitative approach is taken.

As shown in Table 3.1 in the previous section, the effective stiffness term was very significantly overestimated if the walls were loaded at a low axial load eccentricity. To ensure that such results were not significantly skewed (overly sensitive) due to potential inaccuracy in location of applied load such that the reported axial load eccentricities are inexact, in the following Table 3.2 the degree of error which would be induced in the testing results if the reported axial load eccentricities were unprecise is estimated. Namely, in this table the axial load eccentricity is increased by 10 mm and 19.4 mm (the minimum load eccentricity for concentrically loaded walls as prescribed by the Standard, simulating an error of one tenth of the wall thickness which is 194 mm), respectively. The final two columns in the table show the degree of error as a percentage for the induced additional 10 mm and 19.4 mm errors respectively.

Table 3.2 Hatzinikolas et al. (1978b) Testing Program Calculated Lateral Deflection (Using CSA S304-14) vs. Calculated Lateral Deflection with Induced Inaccuracy of Load Eccentricity (Using CSA S304-14)

Wall Name	Slend. Ratio (m/m)	Reinf. (Imp.)	Eccen-tricity (e_{test}) (mm)	Calc. Defl. (mm)	Calculated Deflection With Induced Inaccuracy of Load Eccentricity		**% Error Caused by Induced Inaccuracy of Load Eccentricity**	
					e_{test} + 10 mm	e_{test} + 19.4 mm	e_{test} + 10 mm	e_{test} + 19.4 mm
A1	13.8	Plain	19.4*	25.4	32.0	50.8	**25.9**	**100.0**
A2	13.8	Plain	32.3	16.5	19.1	26.4	**15.5**	**59.8**
A3	13.8	Plain	64.5	13.8	14.9	18.0	**7.8**	**29.9**
A4	13.8	Plain	19.4*	18.9	23.8	37.8	**25.9**	**100.0**
A5	13.8	Plain	76.2	4.8	5.1	6.0	**6.6**	**25.3**
B1	13.8	3#9	19.4*	655.7	825.5	1311.3	**25.9**	**100.0**
B2	13.8	3#9	32.3	110.5	127.6	176.6	**15.5**	**59.8**
B3	13.8	3#9	64.5	37.7	40.7	49.0	**7.8**	**29.9**
B4	13.8	3#9	76.2	52.0	55.4	65.2	**6.6**	**25.3**
B5	13.8	3#9	88.9	39.3	41.6	47.9	**5.6**	**21.7**
C1	15.9	3#9	19.4*	37.3	46.9	74.6	**25.9**	**100.0**
C2	15.9	3#9	19.4*	26.2	32.9	52.3	**25.9**	**100.0**
C3	15.9	3#9	32.3	127.1	146.8	203.1	**15.5**	**59.8**
C4	15.9	3#9	64.5	49.1	52.9	63.8	**7.8**	**29.9**
C5	15.9	3#9	76.2	56.1	59.8	70.3	**6.6**	**25.3**
C6	15.9	3#9	88.9	41.5	43.9	50.5	**5.6**	**21.7**
D1	18.0	3#9	19.4*	364.7	459.2	729.4	**25.9**	**100.0**
D2	18.0	3#9	19.4*	39.1	49.3	78.2	**25.9**	**100.0**
D3	18.0	3#9	32.3	143.0	165.13	228.5	**15.5**	**59.8**
D4	18.0	3#9	64.5	59.0	63.5	76.6	**7.8**	**29.9**
D5	18.0	3#9	76.2	55.1	58.7	69.1	**6.6**	**25.3**
D6	18.0	3#9	88.9	52.7	55.7	64.2	**5.6**	**21.7**
H1	18.0	3#6	19.4*	54.7	68.9	116.0	**25.9**	**112.0**
H2	18.0	3#6	32.3	56.5	68.3	109.2	**20.9**	**93.3**
H3	18.0	3#6	64.5	157.5	209.0	747.1	**32.7**	**374.4**

H4	18.0	3#6	76.2	134.1	174.2	549.0	**29.9**	**309.4**
H5	18.0	3#6	88.9	181.2	252.5	358.1	**39.3**	**97.6**
I1	18.0	3#3	19.4*	41.7	52.5	90.8	**25.9**	**117.9**
I2	18.0	3#3	32.3	47.2	58.3	100.7	**23.5**	**113.2**
I3	18.0	3#3	64.5	82.2	114.6	865.7	**39.4**	**952.9**
I4	18.0	3#3	76.2	67.8	97.6	118.5	**44.0**	**74.8**
I5	18.0	3#3	88.9	110.7	230.6	619.7	**108.3**	**459.9**
L1	24.3	3#9	19.4*	71.3	89.8	142.7	**25.9**	**100.0**
L2	24.3	3#9	32.3	42.6	49.2	68.1	**15.5**	**59.8**
L3	24.3	3#9	64.5	142.7	153.7	185.4	**7.8**	**29.9**
L4	24.3	3#9	76.2	124.9	133.1	156.5	**6.6**	**25.3**
L5	24.3	3#9	88.9	120.2	126.9	146.2	**5.6**	**21.7**
M1	24.3	Plain	19.4*	95.8	120.6	191.5	**25.9**	**100.0**
M2	24.3	Plain	32.3	87.1	100.6	139.3	**15.5**	**59.8**

*In this case axial load was applied concentrically, but as per CSA S304-14 (2014) a minimum eccentricity of 19.4 mm (0.1t) is assumed for the calculation. Haztinikolas et al. (1978a) used blocks with a 194 mm thickness (the old nominal 8 inch blocks (actual width 7⅝ inches)) - such blocks are not commonly used in Canada today.

As may be seen in Table 3.2, the degree of error rises at an increasing rate as the axial load eccentricity is exceeded by an additional distance. This error would be further exaggerated when introduced at originally low axial load eccentricities. However, even when the axial load eccentricity is increased by one tenth of the wall thickness, the error does not exceed the order of magnitude of the original deflection value and thus it is safe to conclude that the very high error in effective stiffness calculation (observed in Section 3.2) at low load eccentricities (such as e = 32.3 mm for most walls) is not caused by a testing error. As the initial axial load eccentricity is greater (for walls loaded at eccentricities of 64.5 mm or greater), any possible lab testing error would contribute even less to the invalidation of the results presented by Hatzinikolas et al. (1978b).

3.3.2 Assessing the Ramifications of the Minimum Axial Load Eccentricity Provision

As per CSA S304-14 (2014), Clause 10.7.2, a minimum eccentricity of one tenth of the wall thickness (0.1t) is used to determine the minimum primary moment which must be used for the determination of the secondary moment effects (if the original factored moment due to axial or lateral load does not already result in a moment greater than the moment from the axial load acting on the wall at an eccentricity of 0.1t). In the above analysis of the tested slender concrete block walls, a minimum axial load eccentricity of 0.1t was always used in calculating the deflection for cases where walls were tested with a concentric axial load applied. While this measure is known to induce a significant conservativism to the results, it is worth exploring to what extent the analysis results aimed at informing the degree of error in the Standard calculated effective stiffness term was caused by this conservative provision (the use of a minimum axial load eccentricity) compared to error in the equation itself. In Table 3.3, two calculated (using the Standard) lateral deflection values are shown for each wall; one when the minimum axial load eccentricity is the Standard-mandated 0.1t and the other when the minimum axial load eccentricity used is a ten times smaller value, 0.01t. The 0.01t eccentricity value was assumed to be more appropriate assuming concentric load was really applied in the tests to within an accuracy of 2 mm (considering a wall thickness of 194 mm).

Table 3.3 Hatzinikolas et al. (1978b) Recorded test Lateral Deflection vs. Calculated Lateral Deflection Using CSA S304-14 (2014) for Concentrically Loaded Walls

Wall Name	Slend. Ratio	Reinf.	Eccent-ricity = t/10	Eccent-ricity = t/100	Recorded Test Deflection	Calculated Deflection		**Calculated/ Test Deflection Ratio**	
	(m/m)	(Imp.)	(mm)	(mm)	(mm)	e=19.4 (mm)	e=1.94 (mm)	**e=19.4 (mm)**	**e=1.94 (mm)**
A1	13.8	Plain	19.4	1.94	1.3	25.4	2.54	**19.5**	**2.0**
A4	13.8	Plain	19.4	1.94	1.0	18.9	1.89	**18.9**	**1.9**
B1	13.8	3#9	19.4	1.94	4.0	655.7	65.57	**163.9**	**16.4**
C1	15.9	3#9	19.4	1.94	1.0	37.3	3.73	**37.3**	**3.7**
C2	15.9	3#9	19.4	1.94	1.0	26.2	2.62	**26.2**	**2.6**
D1	18.0	3#9	19.4	1.94	2.5	364.7	36.47	**145.9**	**14.6**
D2	18.0	3#9	19.4	1.94	3.3	39.1	3.91	**11.9**	**1.2**
H1	18.0	3#6	19.4	1.94	0.1	54.7	5.47	**1215.9**	**121.6**
I1	18.0	3#3	19.4	1.94	0.1	41.7	4.17	**1042.2**	**104.2**
L1	24.3	3#9	19.4	1.94	15.0	71.3	7.13	**4.8**	**0.5**
M1	24.3	Plain	19.4	1.94	5.0	95.8	9.58	**19.2**	**1.9**

As may be read from the table above, the ratios of the calculated to the test deflections for walls which are loaded concentrically are generally unreasonably high when the Standard-mandated minimum axial load eccentricity of 19.4 mm is used; whereas ratios of the calculated to the test deflections are typically closer to a value of 1 when an axial load eccentricity of 1.94 mm is used, indicating that such a minimum axial load eccentricity gives a more accurate approximation of possible error. While it is impossible to know the degree of error present in the lab as the testing program was being carried out, it can be concluded that any absurdly high calculated to tested deflection ratio values are caused by the minimum eccentricity provision in the Standard and not the current effective stiffness equation (Table 3.3 does not assess the degree to which the effective stiffness equation is really conservative at very low axial load eccentricities). It is important to note that this is not a recommendation to remove this minimum axial load eccentricity from the Standard, as a lab environment is not reflective of the realities of construction practices.

3.4 Predicting the Actual Wall Stiffness

As was demonstrated in Section 3.2, the effective stiffness term is being significantly underestimated particularly for walls for which incremental axial load is applied at a low eccentricity. In this work it was concluded that axial load eccentricity must more adequately be considered in the prediction of the wall's effective stiffness term. It is also postulated that effective stiffness depends on the magnitude of the applied axial load itself, and so in this analysis the actual stiffness (the value of the stiffness which corresponds to a particular deflection at a particular load step) is calculated as the slender walls are being incrementally loaded. The desired outcome of the analysis is to understand better how effective stiffness depends on the applied load and additionally to assess to what extent a wall's effective stiffness at failure depends on a wall's slenderness ratio.

As part of the very detailed testing programs results published by Hatzinikolas et al. (1978b), plots representing the lateral deflection profile at each axial load increment of each tested slender wall were used in this analysis. As each wall had been tested to failure over multiple load increments, the plots showed the deflection of the wall at each load increment. This allowed for the stiffness (EI) to be back-calculated at each load increment using the relationship between the lateral deflection of the wall, the secondary moment and the stiffness. The actual stiffness was iterated for at each load increment such that the calculated lateral deflection matched the lateral deflection reported by Hatzinikolas et al. (1978b) for a particular wall. This analysis also allows for the rate at which a wall's effective stiffness is decreasing to be understood; as lateral deflection caused by the initial axial load eccentricity contributes to a secondary moment, the wall cracks and its second moment of area decreases, which causes a decrease in the wall's effective stiffness. The stiffness of the wall at each load step could then be graphed against the applied axial load on the wall.

Figures 3.1-3.6 show graphs of the relationship between the applied axial load (normalized over the critical axial buckling load for each wall) and the realistic wall stiffness. A general trend is observed where the stiffness of the wall first drops rapidly and then more gradually until failure is reached. Note that only the walls loaded in single curvature were studied in the figures below.

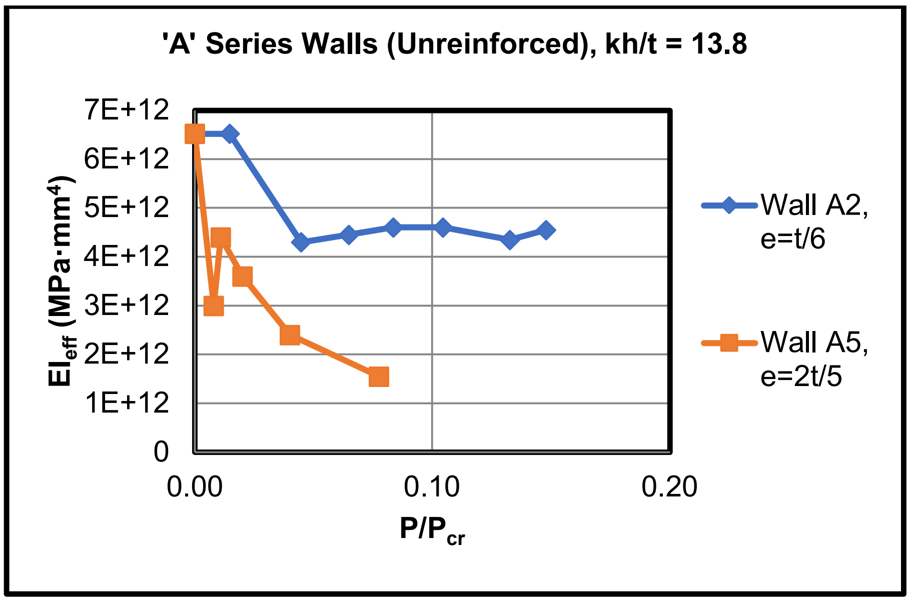

Figure 3.1 P/P_{cr} vs. EI_{eff} Plot – Hatzinikolas et al. (1978a) Program Wall Series 'A'

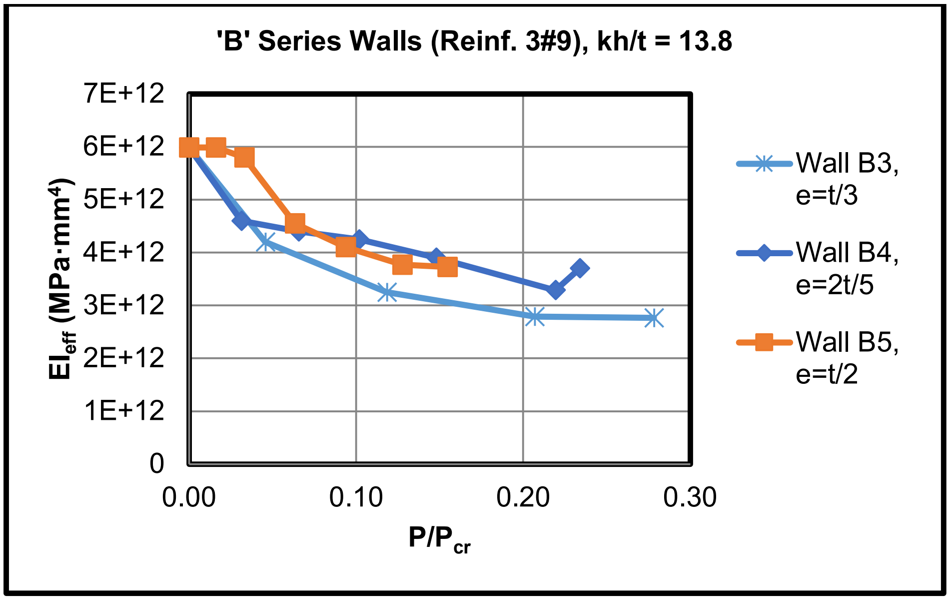

Figure 3.2 P/P_{cr} vs. EI_{eff} Plot – Hatzinikolas et al. (1978a) Program Wall Series 'B'

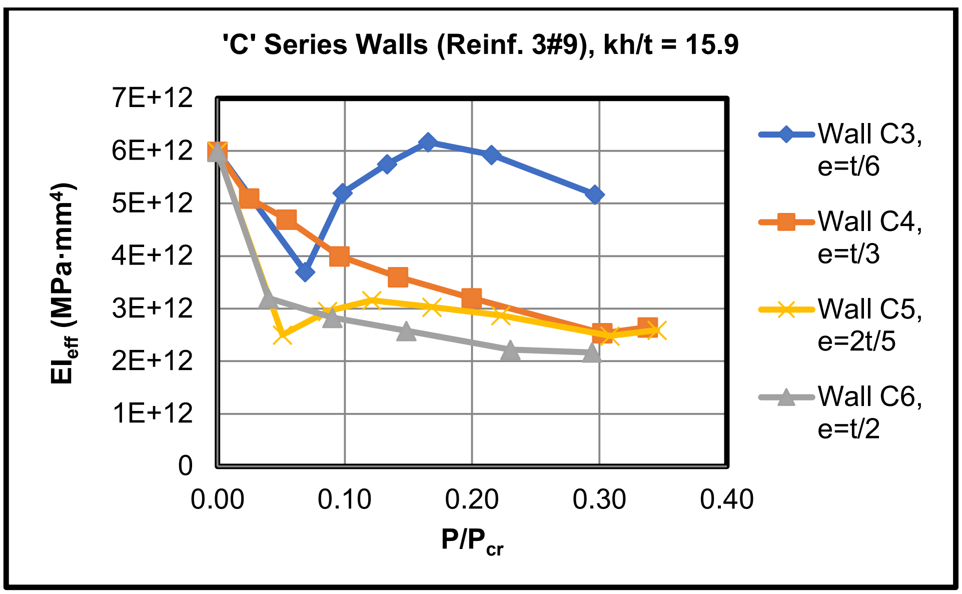

Figure 3.3 P/P_{cr} vs. EI_{eff} Plot – Hatzinikolas et al. (1978a) Program Wall Series 'C'

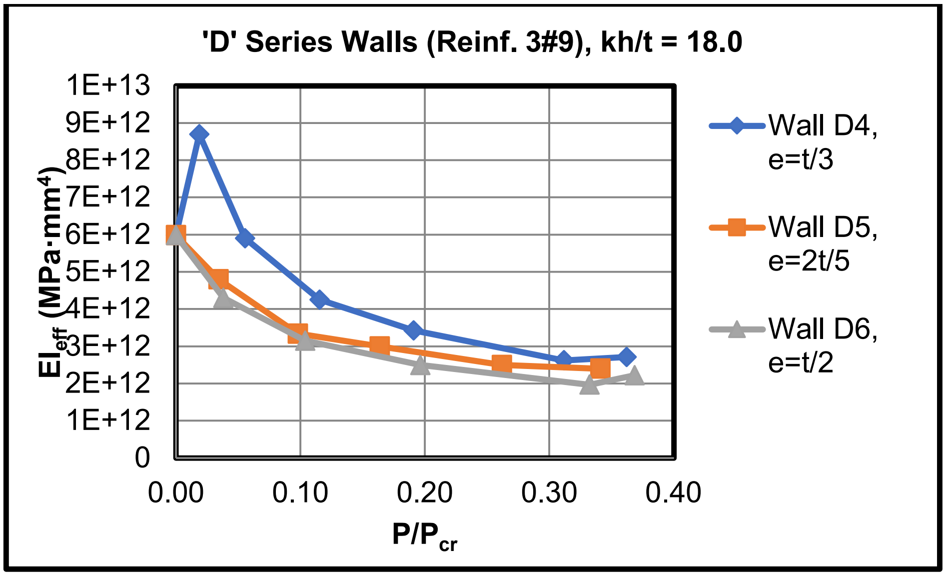

Figure 3.4 P/P_{cr} vs. EI_{eff} Plot – Hatzinikolas et al. (1978a) Program Wall Series 'D'

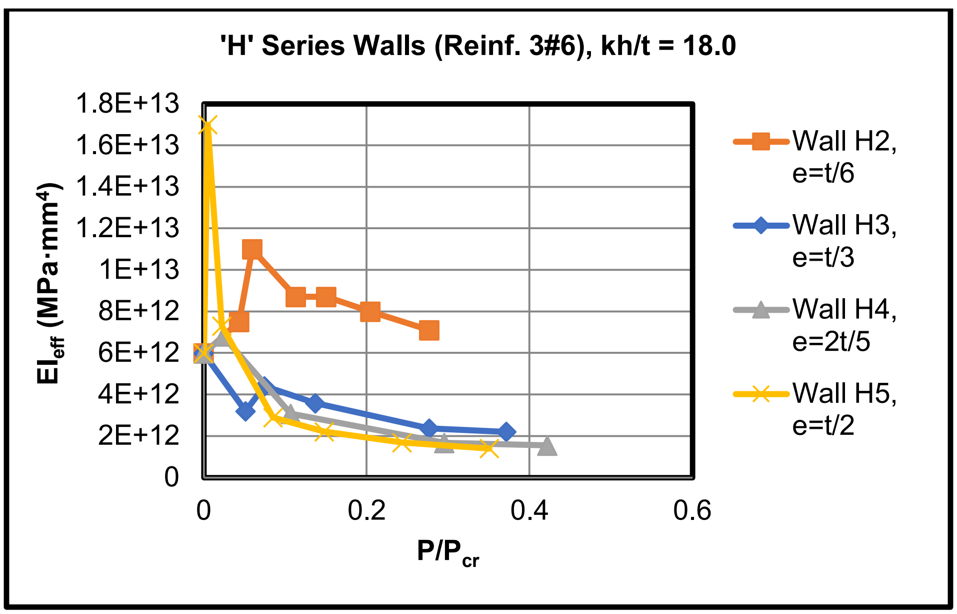

Figure 3.5 P/P_{cr} vs. EI_{eff} Plot – Hatzinikolas et al. (1978a) Program Wall Series 'H'

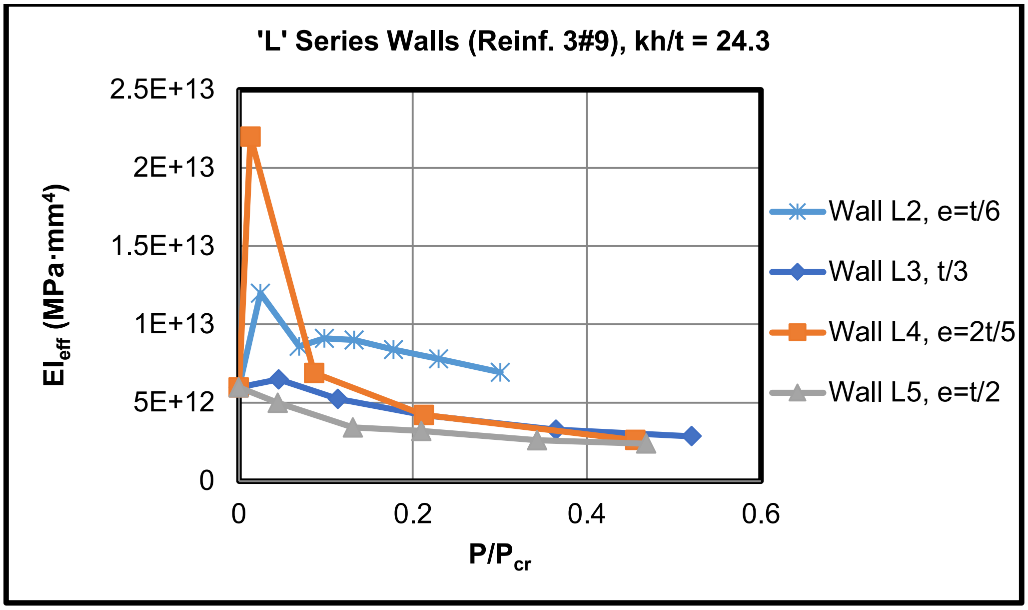

Figure 3.6 P/P_{cr} vs. EI_{eff} Plot – Hatzinikolas et al. (1978a) Program Wall Series 'L'

Wall responses were also plotted in groups based on the axial load eccentricities to which the walls were subjected. In these plots, the normalized axial load was plotted against the stiffness normalized over the original wall stiffnesses (calculated with the elastic modulus and the second moment of area of the uncracked wall cross-section).

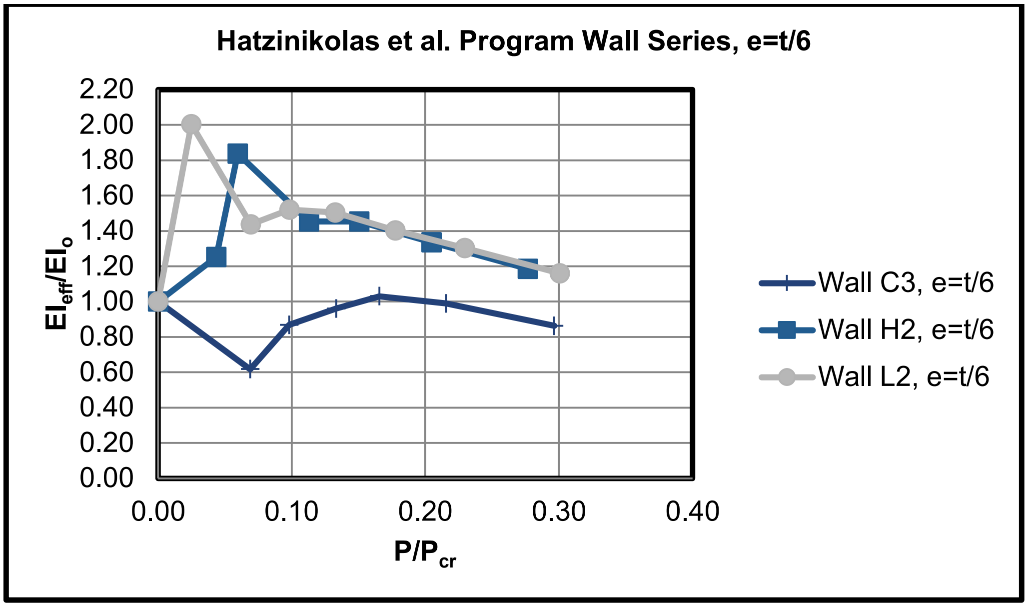

Figure 3.7 P/P_{cr} vs. EI_{eff}/EI_o Plot for Walls Loaded at an Axial Load Eccentricity of t/6

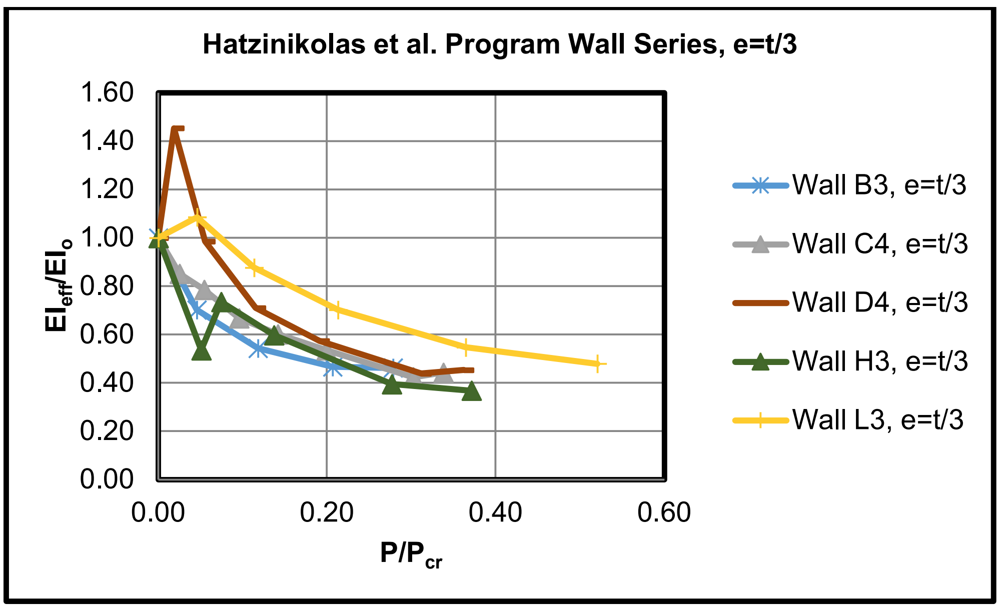

Figure 3.8 P/P_{cr} vs. EI_{eff}/EI_o Plot for Walls Loaded at an Axial Load Eccentricity of t/3

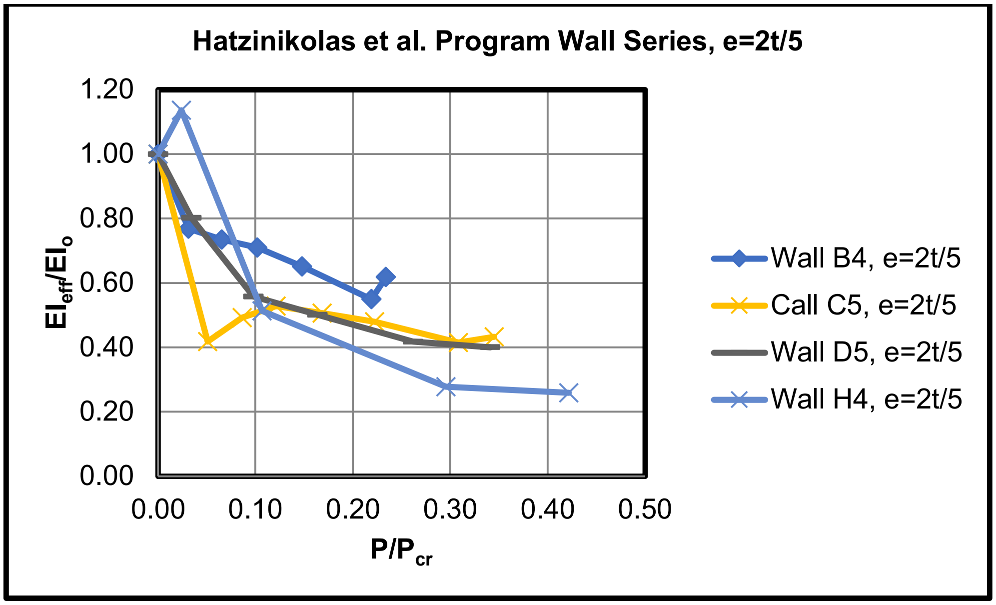

Figure 3.9 P/P_{cr} vs. EI_{eff}/EI_o Plot for Walls Loaded at an Axial Load Eccentricity of 2t/5

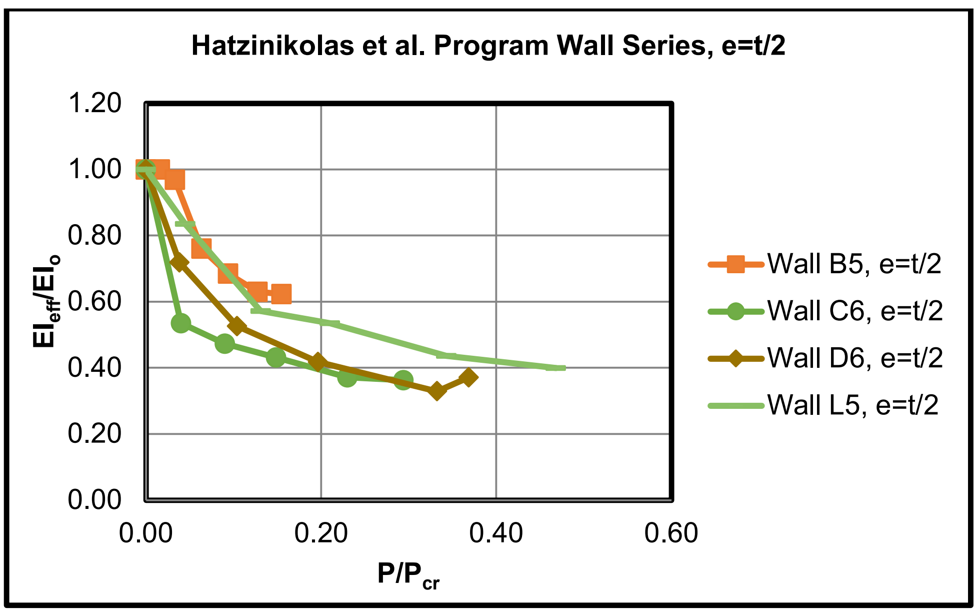

Figure 3.10 P/P_{cr} vs. EI_{eff}/EI_o Plot for Walls Loaded at an Axial Load Eccentricity of t/2

As can be observed in Figures 3.1-3.6, a general trend of the loss of stiffness as a wall is loaded is apparent. The effective stiffness values which the walls approach in each plot can be used to determine a more accurate effective stiffness equation which, as postulated, should depend on the applied axial load, its eccentricity, a wall's material properties and the critical buckling load. An apparent distinction is noticed between the behaviour of unreinforced (Figure

3.1) and reinforced (Figures 3.2-3.6) walls, with unreinforced walls expectedly failing at a significantly lower P/P_{cr} ratio due to their less ductile response.

While walls in Figures 3.1-3.6 were grouped into the same plots based on their slenderness ratios, in Figures 3.7-3.10 the walls were grouped together based on their axial load eccentricities. It can be observed that a wall's axial load eccentricity was a much more significant factor than slenderness ratio in predicting the wall's behaviour. As seen in the plots, the behaviour of walls is more similar when they are loaded at the same axial load eccentricity but built to different slenderness ratios as compared to when they are built to the same slenderness ratio but loaded at different eccentricities. According to the plots in Figures 3.8-3.10, for walls with an applied axial load eccentricity of t/3, 2t/5 and t/2, the final effective stiffness term at failure is generally lower as the axial load eccentricity is greater.

A unique response can be observed in the plots of walls C3, H2 and L2 (all three loaded at an axial load eccentricity of t/6) as compared to the response of all other walls loaded at load eccentricities greater than t/6 (see Figure 3.7). While in the plots of all other walls the effective stiffness term is generally decreasing as load is applied, in the cases of the three aforementioned walls, the effective stiffness term is increasing as the walls are being loaded. In addition, in all three cases the effective stiffness value is even increasing above the original stiffness value, EI_o, before any cracking occurs (exceeding this term is a physical impossibility). These anomalies are explained by the fact that the three walls, all loaded at a low eccentricity, do not deflect much laterally and therefore do not crack significantly. As the three walls do not experience significant lateral deflection, they most likely do not experience a stability failure but rather a material compression failure. Although not stated explicitly for these three walls, Hatzinikolas et al. (1978a) claim that walls loaded concentrically (or nearly concentrically) generally failed due to vertical cracks forming in the grouted cores (indicative of a compression failure) and at similar failure loads to the loads at which equivalent short walls failed (walls with same cross-sectional properties designed to fail at the same compressive strength). This can be taken as additional confirmation that walls C3, H2 and L2 are not failing as slender walls are expected to fail (lateral stability failure). In such cases where walls are categorized as slender but do not fail as a slender wall is expected to fail, the walls would naturally be overdesigned. This issue will be explored further in the “Analysis and Discussion” chapter of this thesis, where the ramifications of incorrect failure mode prediction will be discussed, and alternatives proposed.

3.5 Conclusion

This chapter served as an exploration of the effective stiffness term as defined by the Canadian Standard. The inaccuracy of the effective stiffness equation was demonstrated relative to a wall’s slenderness ratio, axial load eccentricity and applied axial load. In this chapter it was demonstrated that the calculation of the wall effective stiffness was particularly inaccurate at low axial load eccentricities and it was shown that this was not the case due to a lack of precision in the testing, but that the wall behaviour was fundamentally different at such low axial load eccentricities, regardless of the wall’s slenderness (for the range of slenderness ratios in this testing program). Examination of the plots in Figures 3.1-3.10 gives insight into a wall’s actual stiffness as it is incrementally loaded for walls of varying slenderness ratios loaded at varying axial load eccentricities. A significant finding is how different the response was of walls loaded at a low axial load eccentricity as compared to walls loaded at higher axial load eccentricities. In the following “Analysis and Discussion” chapter, this wall behaviour will be made sense of and a new methodology for more accurately calculating the effective stiffness of a masonry wall experiencing secondary moment effects will be proposed.

Chapter 4: Analysis and Discussion

4.1 Introduction

The inaccuracy of the effective stiffness equation as defined in CSA S304-14 (2014) has been brought to light. In this chapter the relationship between the effective stiffness of the wall and the axial load is further explored and an equation is proposed for more effectively estimating the effective stiffness of a wall based on its applied axial load, axial load eccentricity, original stiffness before cracking and critical buckling load. In addition, prompted by the research of Isfeld et al. (2019), the failure mode experienced by walls at various slenderness ratios is explored. The failure modes of walls tested by Hatzinikolas et al. (1978a) are further assessed and modelling conducted by Ahmed et al. (2021) is used to better predict the failure mode of walls based on their slenderness ratio and axial load eccentricity. A two-step process for the prediction of effective stiffness is proposed in which the probable failure mode is first predicted and then the appropriate procedure to determine the secondary moment is applied.

4.2 Proposed Method for Calculation of Effective Stiffness

In the previous chapter the walls' normalized axial loads are plotted against the stiffness normalized to the original wall stiffnesses (calculated with the elastic modulus and the second moment of area of the uncracked wall cross-section). The logical next step was to identify a mathematical relationship between a wall's effective stiffness and the axial load as the wall is incrementally loaded. Doing so could give rise to a more accurate estimation of a wall's effective stiffness as part of the design process, as the current method of calculating a wall's effective stiffness as per the Standard does not consider the load applied to the wall.

The relationship between the normalized axial load and normalized effective stiffness was first identified graphically. Then, employing an iterative approach, an appropriate logarithmic function was chosen such that the algorithm slightly underestimated the effective stiffness for each load increment for a set of walls which had axial load applied at the same load eccentricity but were of varying slenderness ratios. A more sophisticated curve fitting approach was not employed because the aim was to create an equation not to best approximate the values of the effective stiffness term, but rather to conservatively underestimate them at each load increment. Additionally, due to the sample size used for this analysis as well as the lack of variability in material and construction (as only walls used from the Hatzinikolas et al. (1978a) testing program were analyzed), it was deemed sufficient simply to iterate for the most appropriate equation (an equation which just underestimates the effective stiffness values for each load step). A logarithmic function most accurately followed the curve of the relationship between normalized axial load vs. normalized effective stiffness.

The following equation is proposed to estimate the effective stiffness:

$$\frac{EI_{eff}}{EI_o} = -\left(0.05 * \left(\frac{t}{e}\right)\right) \ln\left(\frac{P}{P_{cr}}\right) + 0.2, \quad EI_{eff} \leq EI_o \tag{4.1}$$

where EI_{eff} represents the effective stiffness, EI_o represents the original stiffness of the wall, t represents the wall thickness, e represents the axial load eccentricity, P represents the applied axial load and P_{cr} represents critical buckling load.

Below are shown the three graphs based on which the equation (Equation 4.1) has been developed, showing how the points on the normalized axial load vs. normalized effective stiffness graphs are contained by the curve of the developed equation (shown in black).

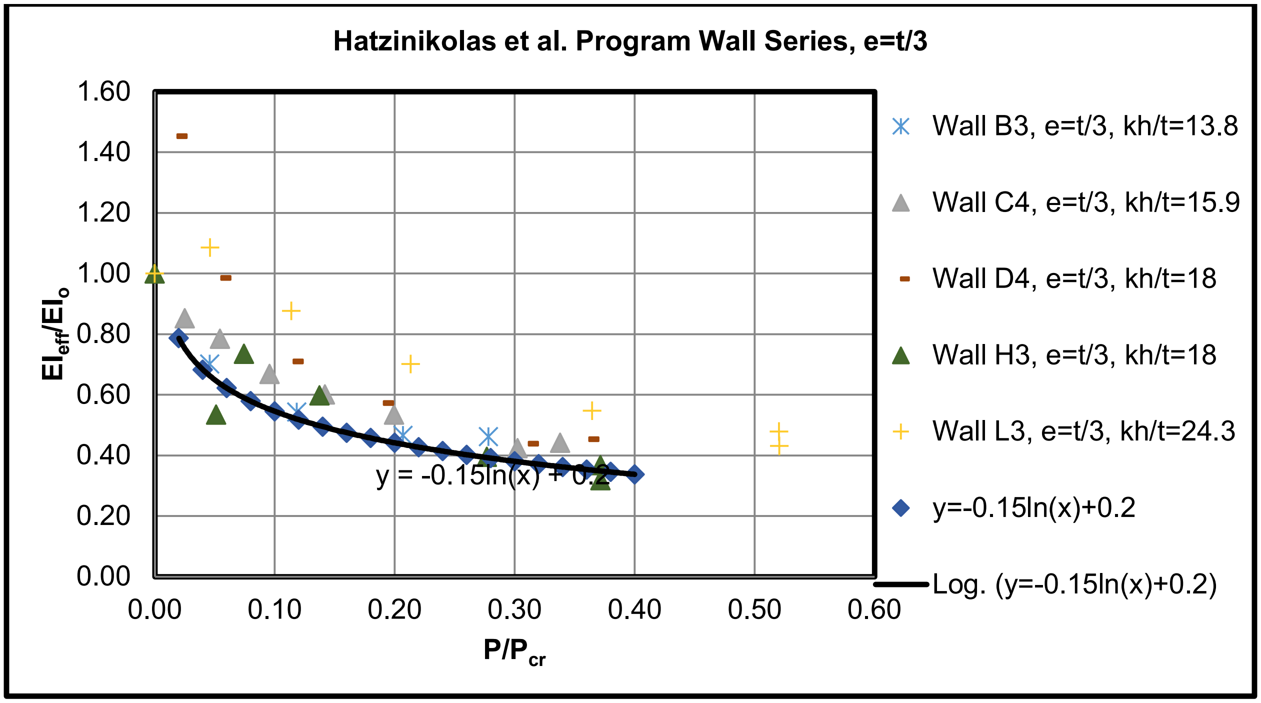

Figure 4.1 P/P_{cr} vs. EI_{eff}/EI_o Plot for Walls Loaded at an Axial Load Eccentricity of t/3

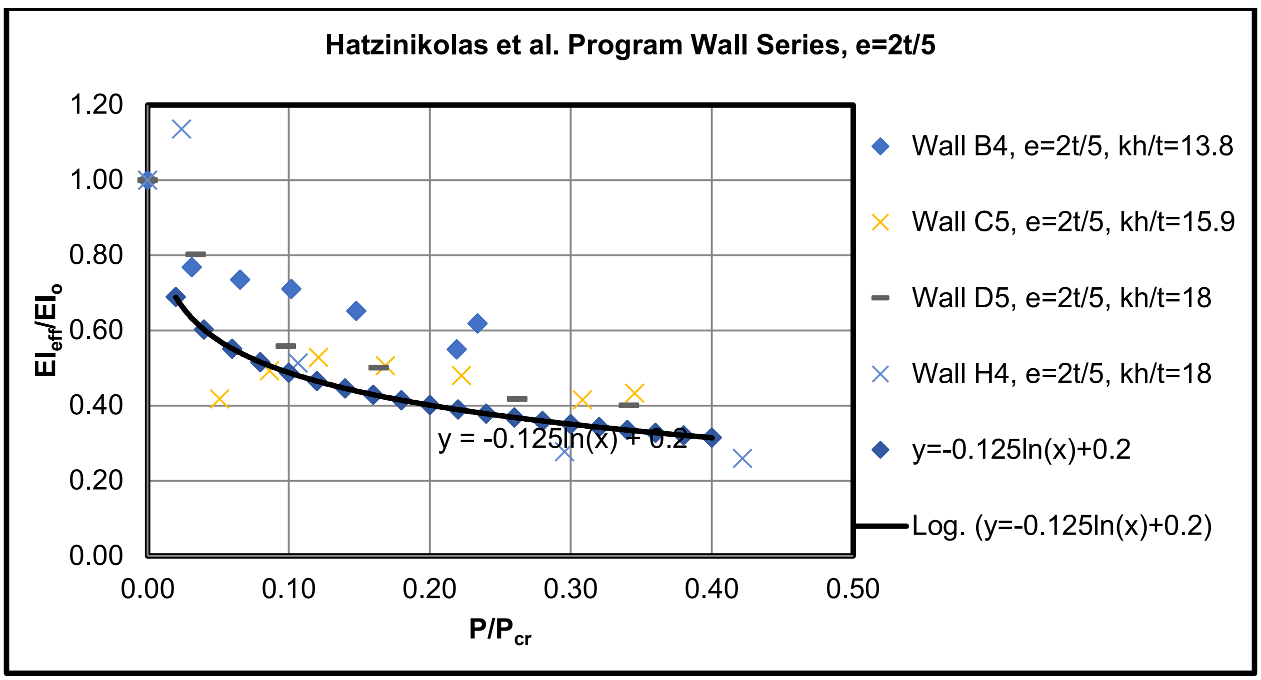

Figure 4.2 P/P_{cr} vs. EI_{eff}/EI_o Plot for Walls Loaded at an Axial Load Eccentricity of 2t/5

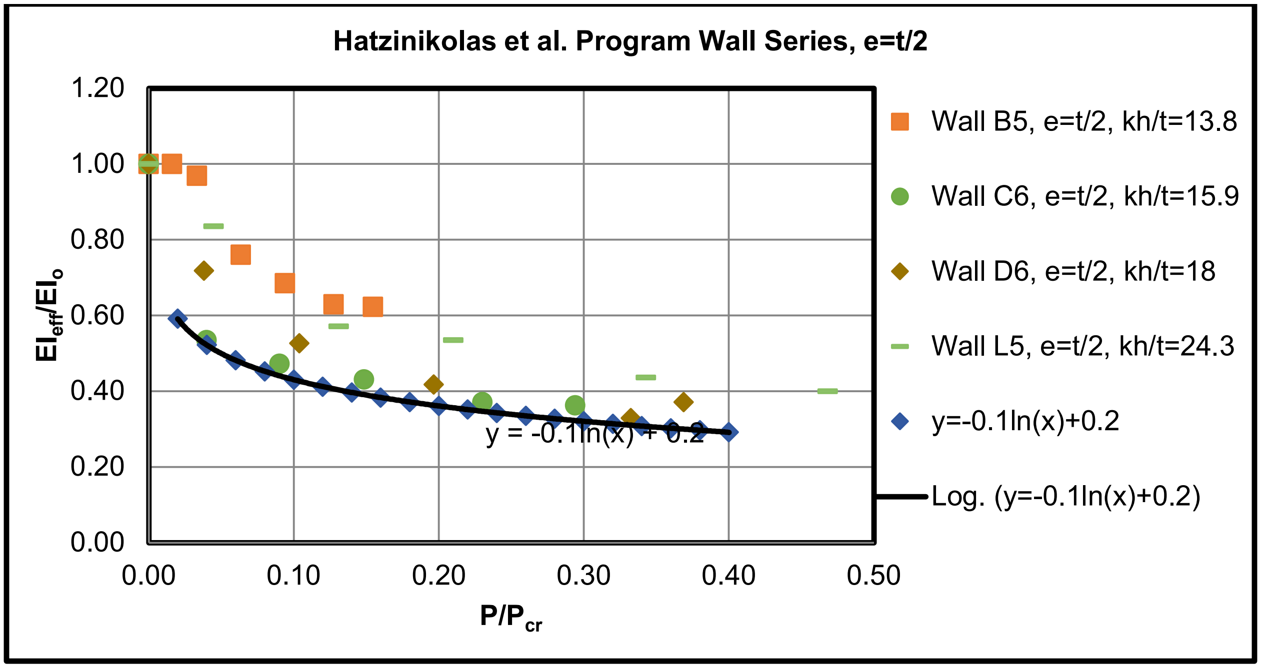

Figure 4.3 P/P_{cr} vs. EI_{eff}/EI_o Plot for Walls Loaded at an Axial Load Eccentricity of t/2

In a potential design procedure, the design load, critical buckling load and the original wall stiffness (Young's modulus and second moment of area before any cracking) would have to be known to back-calculate the effective stiffness of the masonry wall. This effective stiffness should then be used to calculate the secondary moment acting on the wall and thus proceed in the design process.

As shown in the figures above, several of the plotted points are not contained (the points plotted outside of the proposed equation) by the proposed P/P_{cr} vs. EI_{eff}/EI_o functions. These points which are not placed above the proposed curves are seen as outliers and had to be ignored to produce a meaningful equation. There are several limitations to the proposed equations. For instance, these equations have been developed based on the testing program of Hatzinikolas et al. (1978a) and as such reflect the specific testing conditions and materials which were used as part of this program. The above equations will likely need to be adjusted as more data are processed and future experiments are conducted; in particular, the equations should have to be modified as required as a larger number of wall dimensions, slenderness ratios and material properties are assessed. Before such an approach can be considered for design purposes, a greater variety of loading conditions will need to be considered. Namely, while it is presumed that any lateral loads on the wall can be converted to axial loads at a particular eccentricity, these equations must first be assessed relative to a testing program in which slender masonry walls are loaded both laterally and axially.

4.3 Prediction of Slender Wall Failure Mode

Although it is assumed that walls categorized in the Standard as behaving as slender masonry walls should experience an out-of-plane failure, there were several instances where this was not the case. Firstly, as can be observed in the previous chapter in the P/P_{cr} vs EI_{eff}/EI_o graphs, seen in Figure 3.3, Figure 3.5 and Figure 3.6, it is shown that the effective stiffness of walls C3, H2 and L2, which are all loaded at an axial load eccentricity of t/6, increased as the walls were loaded and never decreased to the level of the effective stiffness of other walls which all experienced an out-of-plane failure. Notably, the effective stiffness in all three cases even increased above the original stiffness value, EI_o, from which it can be concluded that the walls did not experience significant bending as they were being loaded. Hatzinikolas et al. (1978a) noted that certain walls which according to the Canadian Standard today should behave as slender walls and experience stability failure in fact failed by compression failure (such as Wall B2, see vertical cracks in Figure 4.4). It is additionally noted in the results of the testing program that the walls did not experience significant lateral deflection. These facts suggest, as would be expected theoretically, that the failure mode of an axially loaded wall depends not only on its slenderness ratio, but also on the axial load eccentricity.

Figure 4.4 Hatzinikolas et al. (1978a) Program Wall B2 (e=t/6) Failing in Compression

This hypothesis that slender walls typically experience a compression failure when loaded at a low enough axial load eccentricity was proposed by Isfeld et al. (2019). Isfeld et al. (2019) modelled unreinforced concrete block walls of various slenderness ratios (from height to thickness ratio of 5 to ratio of 60) and categorized the walls based on failure mode. Specifically, wall failure mode was distinguished based on the bed joints being open, closed or partially closed at failure, as shown in the Figure 4.5 below (copied from Isfeld et al. (2019)).

Wall h/t	Fix-Fix	Pinned Support Eccentricity e/t						
		0	1/10	1/6	1/4	1/3	1/2.5	1/2
5	0	0	1.2	1.8	2.2	2.3	2.6	2.8
10	0	0	2.1	3.2	4.1	6.8	5.3	1.7
20	0	0	8.8	12.6	12.2	13.9	13.9	0.1
30	0	0	17.1	21.0	22.4	22.9	22.9	2.4
40	0	3.7	29.5	38.4	38.9	38.9	24.2	0.3
60	0	33.9	78.7	78.5	61.7	45.5	23.8	0.7

All bed joints fully closed
Bed joints with partial contact
Full opening of some bed joints

Figure 4.5 Masonry Wall Failure Mode, Copied from Isfeld et al. (2019)

Notably, as per the study, walls up to a slenderness ratio of 60 at an axial load eccentricity of one sixth of the wall thickness (t/6) or less failed with bed joints closed, thus demonstrating that slenderness ratio alone is not indicative of failure mode of a wall. As per the same table published by Isfeld et al. (2019), walls loaded at an axial load eccentricity of one fourth of the wall thickness (t/4) or higher fail with open or partially open bed joints. Walls tested in the Hatzinikolas et al. (1978a) testing program had seemingly followed the same pattern of failure modes, with walls loaded at an axial load eccentricity of one sixth of the wall thickness (t/6) evidently experiencing a distinct failure mode, as can be seen in Figure 3.7 in the previous chapter and as copied here below (in Figure 4.6). The fact that the effective stiffness of the walls shown below increases as the wall is being loaded is indication enough that the wall cross-section is not experiencing significant reduction, further indicating that these walls are not experiencing a lateral stability failure. The recorded "increase" in stiffness is probably due to the very small lateral displacements being in the noise of such readings – small changes in the measurement having a large effect on the apparent stiffness. The failure modes predicted based on the P/P_{cr} vs. EI_{eff}/EI_o plots for several of the wall series tested by Hatzinikolas et al. (1978a) are summarized in Table 4.1 (a similar table was not produced for results published by Yokel et al. (1970) due to the significant number of local failures recorded, as noted in Section 2.4.1 in the "Literature Review" chapter).

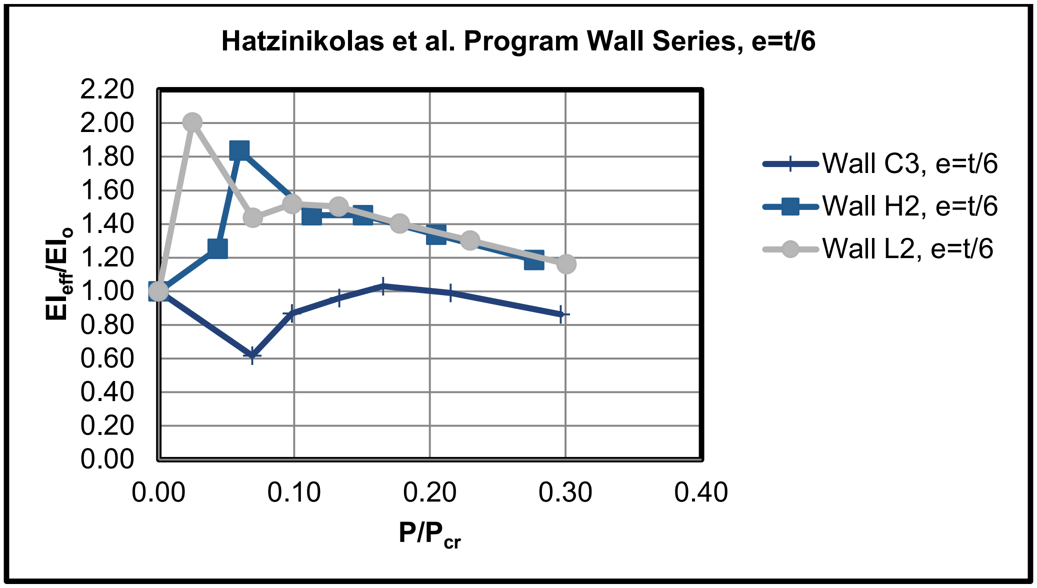

Figure 4.6 P/P$_{cr}$ vs. EI$_{eff}$/EI$_o$ Plot for Walls Loaded at an Axial Load Eccentricity of t/6

Table 4.1 Predicted Failure Mode Based on Slenderness Ratio and Eccentricity - Hatzinikolas et al. (1978b) Data Analyzed

Hatzinikolas et al. (1978a) Wall Series	h/t	Predicted Failure Mode Based on Hatzinikolas et al. (1978b) Results				
		e = 0	e = t/6	e = t/3	e = 2t/5	e = t/2
C	15.9	Compression	Compression	Flexure	Flexure	Flexure
H	18.0	Compression	Compression	Flexure	Flexure	Flexure
L	24.3	Compression	Compression	Flexure	Flexure	Flexure

As per the above findings, it is evident that particular walls which would be predicted to be experiencing slenderness effects by the Canadian Design Standard are in fact failing in compression, leading to a significant overdesign. As per the current CSA S304-14 (2014) design procedure, the walls in Table 4.1 which are here predicted to be failing in compression would themselves be designed as if they are expected to experience significant lateral deflection, which is reflected in the effective stiffness term used in the calculation of the secondary moment experienced by a wall. However, the realization that slender walls loaded at a low axial load eccentricity are in fact failing in compression allowed for the development of the iterative effective stiffness equation presented above (Equation 4.1 presented in Section 4.2), since only the walls which are expected to fail in flexure (walls loaded at higher axial load eccentricity) will experience significant lateral deflection and thus experience a significant decrease in effective stiffness. It would be beneficial in the design process to break down slender walls into categories based on their expected failure mode (as shown in Table 4.1), as estimating an effective stiffness term is only useful for walls which will fail in flexure. Such a breakdown had not been proposed in previous testing programs and studies despite the fact that walls loaded at low axial load eccentricities appeared to fail in compression (such as walls C3, H2 and L2 noted in Figure 4.6 above).

The differences in behaviour of walls loaded to failure at varying axial load eccentricities and slenderness ratios are further analyzed and shown in the Figures 4.7-4.12 below. In each figure, the moment resistance vs. axial load resistance interaction diagram is plotted for the wall cross-section for each wall series tested by Hatzinikolas et al. (1978b). The applied axial loads (at each load step) and corresponding total moments resisted (including secondary moment) for each tested wall are also plotted on each figure up until the failure load was reached. As these total moments are calculated by multiplying the total applied axial load (at each load step) with the corresponding recorded maximum lateral deflection (as recorded by Hatzinikolas et at. (1978b)), these M vs. P plots are reflective of the deflection recorded at each load step and thus the change in the slope along each M vs. P curve can be used to indicate the degree to which secondary moment effects are occurring (as the load step is kept consistent in magnitude for a particular test). For the purpose of this analysis, the axial and moment resistance envelope values were calculated without accounting for strength reduction factors, as laboratory test specimens were being considered. As shown in the figures below, there is generally agreement between the interaction diagram and the failure loads reported by Hatzinikolas et al. (1978b).

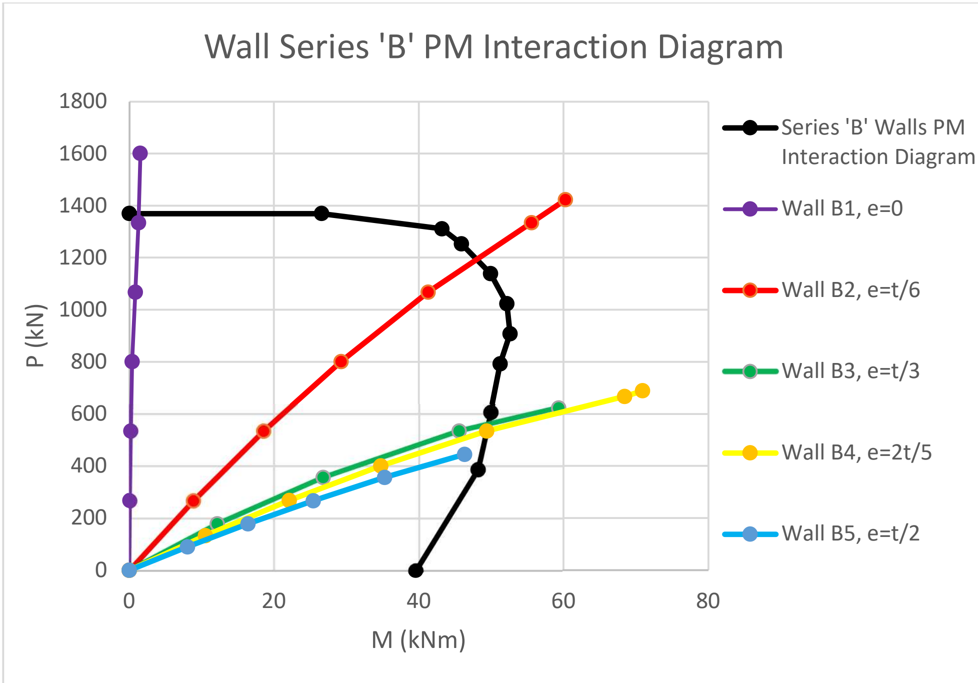

Figure 4.7 Wall Series 'B' Interaction Diagram, h/t = 13.8, 3#9 Vert. Reinf. Bars (Imp.) – Applied Moment vs. Applied Axial Load Plotted at Each Load Step as per Hatzinikolas et al. (1978b)

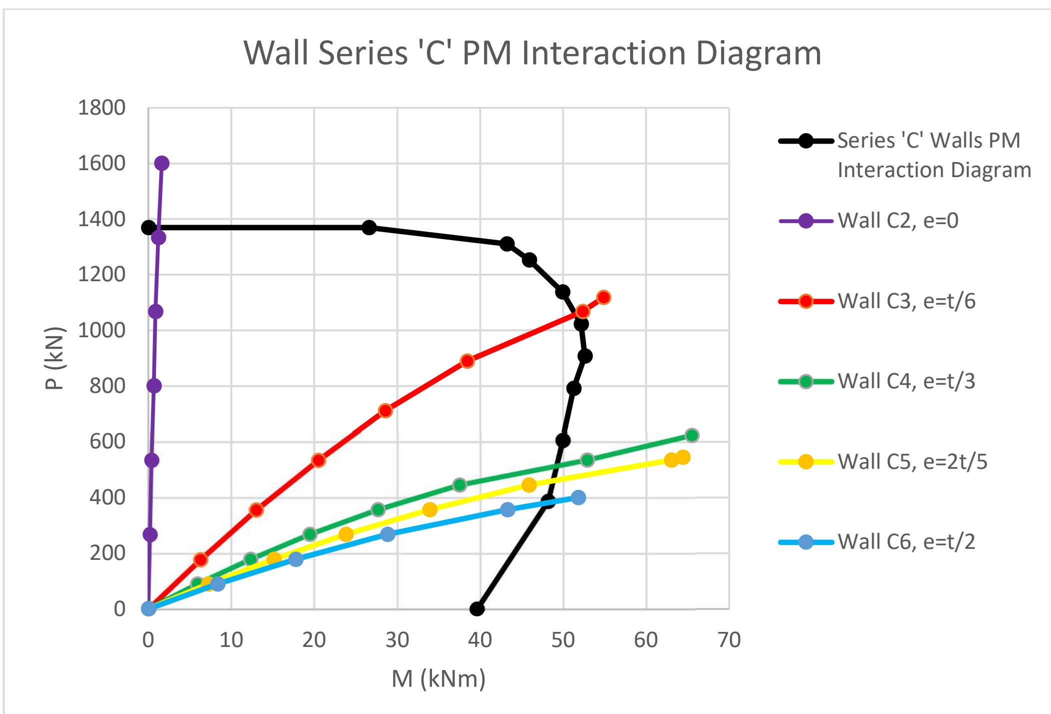

Figure 4.8 Wall Series 'C' Interaction Diagram, h/t = 15.9, 3#9 Vert. Reinf. Bars (Imp.) – Applied Moment vs. Applied Axial Load Plotted at Each Load Step as per Hatzinikolas et al. (1978b)

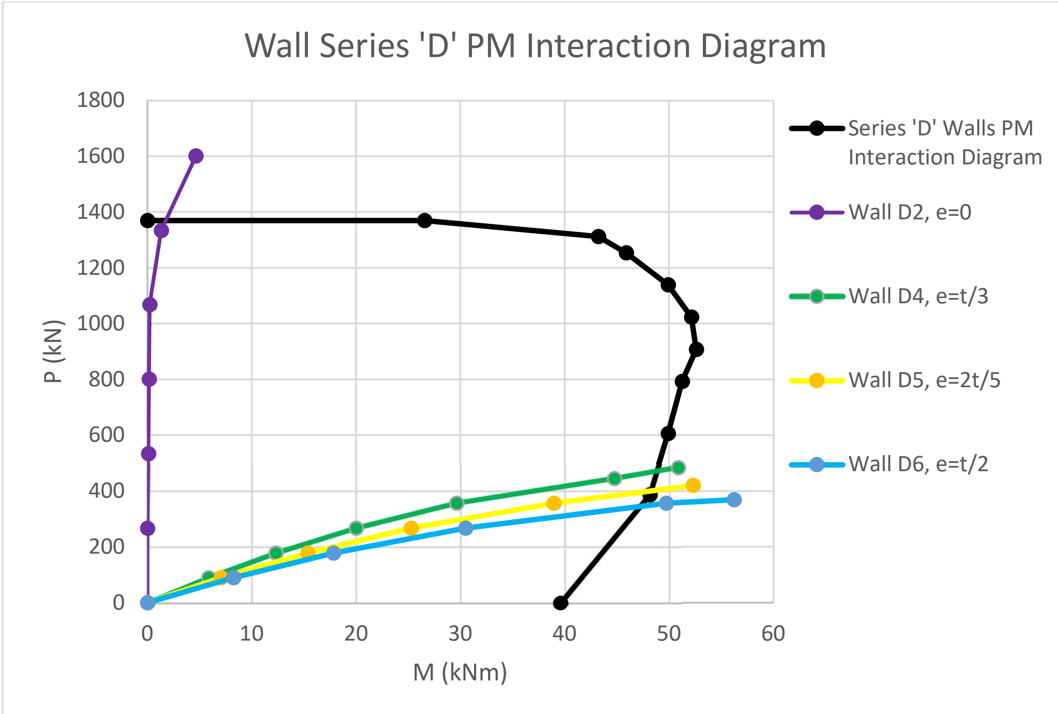

Figure 4.9 Wall Series 'D' Interaction Diagram, h/t = 18.0, 3#9 Vert. Reinf. Bars (Imp.) – Applied Moment vs. Applied Axial Load Plotted at Each Load Step as per Hatzinikolas et al. (1978b)

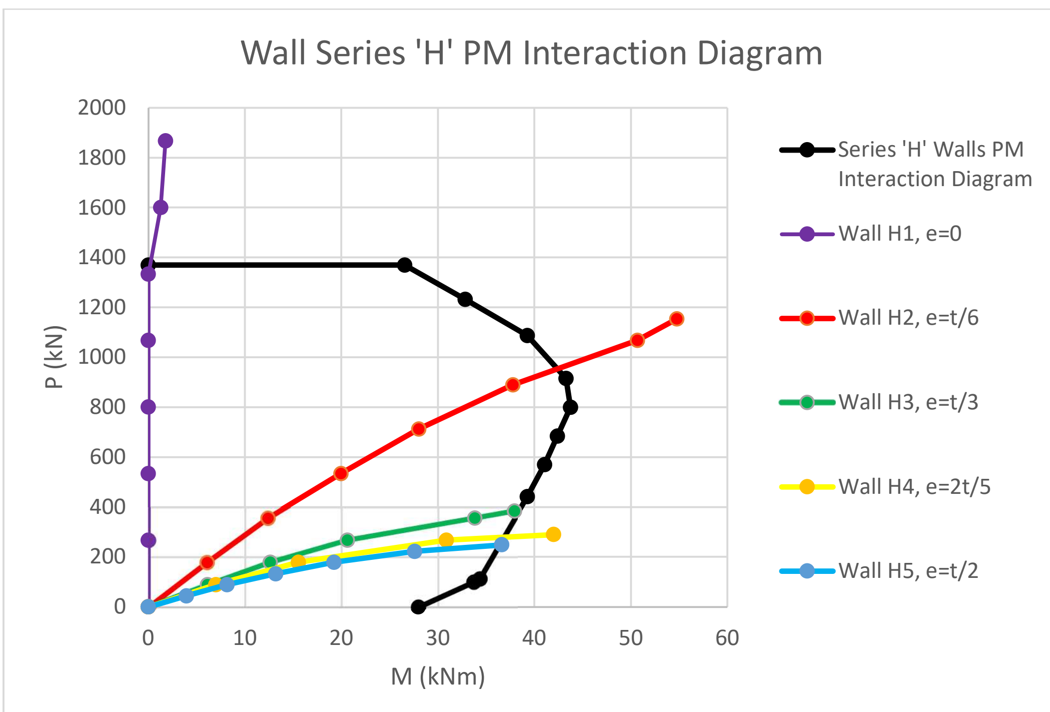

Figure 4.10 Wall Series 'H' Interaction Diagram, h/t = 18.0, 3#6 Vert. Reinf. Bars (Imp.)– Applied Moment vs. Applied Axial Load Plotted at Each Load Step as per Hatzinikolas et al. (1978b)

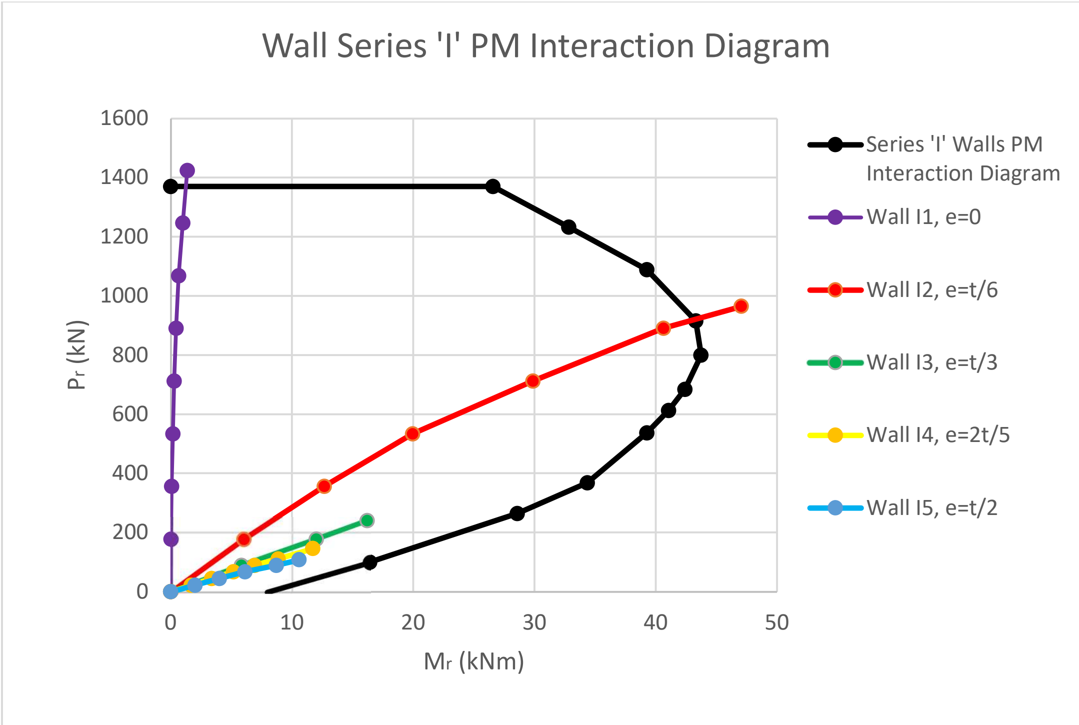

Figure 4.11 Wall Series 'I' Interaction Diagram, h/t = 18.0, 3#3 Vert. Reinf. Bars (Imp.) – Applied Moment vs. Applied Axial Load Plotted at Each Load Step as per Hatzinikolas et al. (1978b)

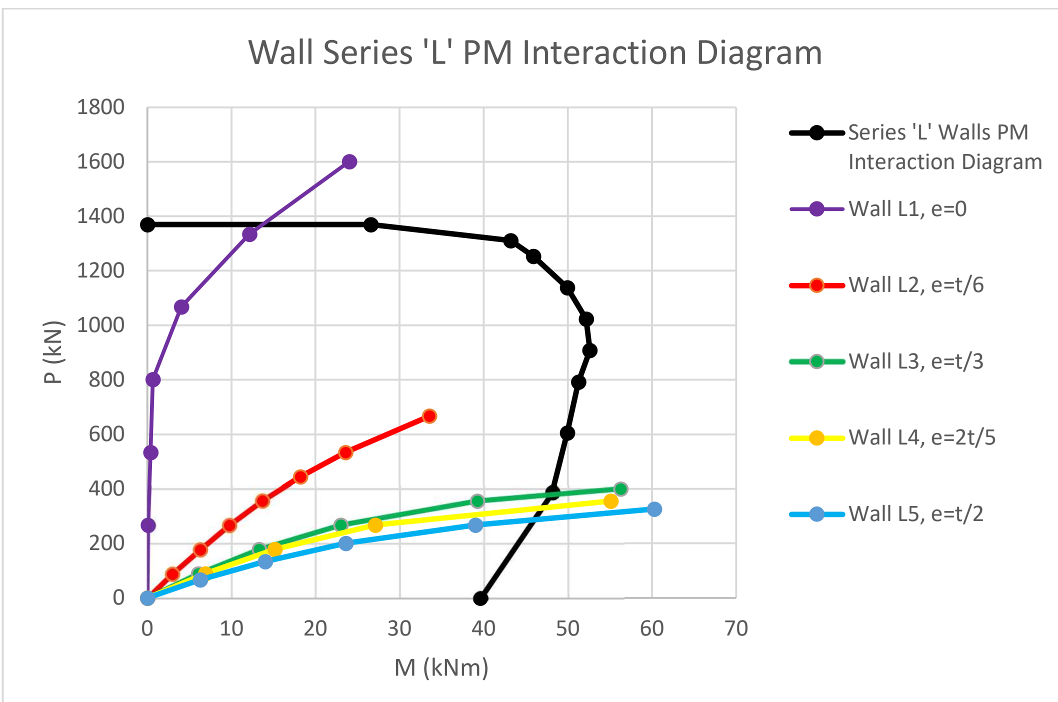

Figure 4.12 Wall Series 'L' Interaction Diagram, h/t = 24.3, 3#9 Vert. Reinf. Bars (Imp.)– Applied Moment vs. Applied Axial Load Plotted at Each Load Step as per Hatzinikolas et al. (1978b)

By observing the figures above, clear patterns are noted which can serve to distinguish between three distinct behaviours for walls loaded at varying axial load eccentricities. Across each of the six figures above, the concentrically loaded walls (B1, C2, D2, H1, I1 and L1) are minimally deflecting and thus the graphs confirm that these walls are experiencing a classical compressive failure. The M vs. P plots for walls of axial load eccentricities of one third of the wall thickness (t/3) or greater (walls B3-B5, C4-C6, D4-D6, H3-H5, I3-I5 and L3-L5) appear to follow a similarly shaped curve within each wall series and generally were recorded to experience predominantly flexural (out-of-plane) failure, as the walls were failing at low axial load as compared to the walls loaded at axial load eccentricities of 0 and one sixth of their thickness (t/6). The third grouping of walls (B2, C3, H2, I2 and L2) are loaded at an axial load eccentricity of one sixth of their thickness (t/6). They generally fail at a high compressive load but are also affected by a large moment and exhibit a behaviour unique from the other two groups of walls. It is evident from the plots above that these walls are experiencing some lateral deflection, though the large moments resisted prior to failure are also predominantly caused by the high axial compressive loads the walls are resisting when loaded at an axial load eccentricity of one sixth their thickness (t/6). It must also be noted walls with a lower height to thickness ratios and a higher vertical steel reinforcement ratio (such as walls B2, C3 and H2) are experiencing failure at loads in the range of their compressive capacities as per the corresponding PM interaction diagram (meaning that the moments resisted did not significantly reduce their axial load capacities and the walls are definitively not experiencing an out-of-plane failure). The failure of wall B2 is shown in Figure 4.4 where it appears to be experiencing a compressive crushing failure (as opposed to an out-of-plane failure), despite the fact that it is shown to be resisting a large applied moment in Figure 4.7. On the other hand, the axial capacity of walls was lower as they were built to a higher slenderness ratio (such as wall L2 built to a ratio of 24.3) despite being loaded at an axial load eccentricity of one sixth of the thickness (t/6). By observing the slopes of the M vs. P plots of the walls loaded axially at one sixth of the thickness (t/6), it is evident that walls built to higher slenderness ratios experience a greater increase in moment resisted at each load step, meaning that these more slender walls are subject to greater secondary moment effects. It is relevant to point out that the behaviour of walls in the C, H and L series loaded at an axial load eccentricity of one sixth of the wall thickness (walls C3, H2 and L2) could best be understood by contrasting Figure 4.6 (which shows their respective P/P_{cr} vs. EI_{eff}/EI_o plots) with Figures 4.8, 4.10 and 4.12 respectively. It is evident that wall L2, loaded at an axial load eccentricity of one sixth of its thickness (t/6) and built to a slenderness ratio of 24.3 does experience some non-negligible secondary moment effects

Figures 4.7-4.12 help to confirm the fact that walls categorized as slender as per the current Canadian Standard are not always expected to fail as such and that a more refined process should be developed in order to distinguish which walls will experience significant secondary moment effects. Due to the limited sample size of walls loaded at each axial load eccentricity, resulting in only one wall of its slenderness ratio being loaded at a particular axial load eccentricity, it is not advisable to draw any direct conclusions other than that up to a certain slenderness ratio and axial load eccentricity walls will not experience significant secondary moment effects. These results should be remembered when future wall testing programs are assessed, as a clear conclusion on the behaviour of walls loaded at low load eccentricities cannot be reached based on the results of the analysis considering a single testing program.

4.4 Influence of Lateral Load on the Failure Mode of Axially Loaded Slender Walls (Published by Ahmed et al. (2021))

It is clear from the results discussed above that the most significant leap in slender wall design efficiency would be to differentiate axially loaded masonry walls based on their expected failure mode before applying a specific design approach. However, this approach would be without application should it be determined that walls in real world situations are readily experiencing significant lateral load and therefore expected to experience out-of-plane failure. For this reason, it was important to assess the typical wind pressure an axially loaded slender wall would experience to predict the influence that lateral load would have on the mode of failure of such walls.

As part of the paper “Examining the Mode of Failure of Slender Concrete Block Walls” by Ahmed et al. (2021) (of which the author of this thesis was a co-author), finite element models of walls with and without lateral loads were produced to assess the degree to which the lateral loads affect the wall failure mode and capacity. For the purpose of the study, the applied lateral loads represented average Canadian wind pressures as per the National Building Code of Canada (2015). The purpose of using the NBCC (2015) was to predict an approximate lateral wind load to which slender walls are exposed. This was done by assessing the design wind pressures for cities across Canada (as per the Code) and taking an average wind pressure value which would serve as an approximation for a typical wind pressure a slender wall may be designed to resist. Unreinforced and ungrouted concrete block walls of four height to thickness ratios (h/t=10, h/t=20, h/t=30 and h/t=40) were modelled as part of the study. In particular, the study focused on wall models which were loaded at low axial load eccentricities to determine whether these walls failed by compressive failure even with the applied lateral load, as would have been expected after reviewing the results from Isfeld et al. (2019) and Hatzinikolas et al. (1978b) above. Wall models were loaded at axial loads eccentricities of 0, one tenth of the wall thickness and one sixth of the wall thickness. Note that most walls tested as part of the Hatzinikolas et al. (1978a) testing program which were loaded at an axial load eccentricity of one sixth of the wall thickness did not experience a significant reduction in stiffness and experienced a material (compressive) failure. This is consistent with the theory, given that the region within an eccentricity of one sixth of the wall thickness is considered the kern and pure axial load applied within this eccentricity should only lead to a compressive failure. The results of the study are summarized in Table 4.2 below.

Table 4.2 Joint Status at Failure for Walls With and Without Average Out-of-Plane Wind Load (Copied from Ahmed et al. (2021))

h/t	Joint Status at Failure					
	e=0		e=t/10		e=t/6	
	No Out-of-Plane Load	Out-of-Plane Load	No Out-of-Plane Load	Out-of-Plane Load	No Out-of-Plane Load	Out-of-Plane Load
10	Closed	Closed	Closed	Closed	Closed	Closed
20	Closed	Closed	Closed	Closed	Closed	Closed
30	Closed	Closed	Closed	Closed	Closed	Closed
40	Closed	Closed	Closed	Closed	Closed	Partial Contact

As shown in the table above, even with the lateral load (average wind load across many locations in Canada) applied to the concrete block walls, the walls generally failed with the bed joints appearing to be closed (except for the wall with a height to thickness ratio of 40 loaded at an axial load eccentricity of t/6). These results support the claim that the procedure for the design of masonry walls experiencing secondary moment effects (walls for which slenderness must be considered) in the Canadian Standard (CSA S304-14 (2014)) could feasibly be reformed such that the wall failure mode is predicted before continuing with design, as slender walls loaded at low eccentricity generally did not demonstrate flexural failure. Initial imperfections in the wall, like a small out-of-plane curvature were not considered in this analysis, and further modelling needs to be done to determine the effect of such imperfections. Single vs. double curvature will also affect the likelihood of compressive failure rather than flexure or buckling instability.

4.5 A Potential Design Approach

4.5.1 Design Summary

As is demonstrated above, slender masonry walls loaded at a low axial load eccentricity without significant lateral applied load are being overdesigned due to the requirement in CSA S304-14

(2014) for a secondary moment to be calculated, even when minimal lateral deflection is expected. The fact that slender walls loaded at low axial load eccentricity are typically failing in compression rather than experiencing out-of-plane failure (as would be expected of slender walls), when considered in conjunction with the above-proposed equation for the calculation of effective stiffness, EI_{eff}, could give rise to a new design approach. As part of this potential design approach, walls could first be identified as either expected to fail in compression or out-of-plane (based on their axial load eccentricities, lateral load magnitude and slenderness ratio), then either designed without consideration of secondary moment or simply designed as slender walls (with the refined effective stiffness equation used, see Equation 4.1). The following is a summation of this proposed potential design procedure for slender masonry walls.

Step 1: First, the wall failure mode is to be predicted. Based on the applied axial load eccentricity, the wall slenderness ratio, and the magnitude of applied lateral load, it should be predicted whether a particular wall will experience material or out-of-plane failure. While the exact slenderness ratio, axial load eccentricity and lateral load limits past which walls are expected to experience slenderness effects have not been set as part of this thesis (these exact limits must be defined based on future research), for the purpose of this example, Table 4.2 (the results from the Ahmed et al. (2021) study) will be used to predict the failure mode. As per Table 4.2, walls loaded at an axial load eccentricity of one sixth of the wall thickness (t/6) or less and either built to a slenderness ratio of 40 without an applied lateral load or built up to a slenderness ratio of 30 with a maximum applied lateral pressure of 0.45 kPa should fail with their bed joints closed (indicating a material failure).

Step 2a: If the wall slenderness ratio, applied axial load eccentricity and applied lateral load fall within the limits of a wall expected to experience a material failure, secondary moment does not need to be considered (as the wall is not expected to crack significantly and thus wall stiffness will not be reduced significantly due to flexural cracking). Rather, the wall section is to be designed to resist the applied axial load and initial applied moment. A P-M interaction failure envelope should then be developed for a proposed wall design to ensure the wall can resist the applied loads.

Step 2b: If, however, the wall is predicted to experience out-of-plane failure based on the slenderness, applied axial load or lateral load exceeding the above-defined limits, secondary moment is to be calculated. Either the moment magnifier or the load displacement method is to be used to determine the secondary moment, though the effective stiffness, EI_{eff}, a required input, is to be calculated as per this proposed equation (Equation 4.1, as explained above in Section 4.2):

$$\frac{EI_{eff}}{EI_o} = -(0.05 * (\frac{t}{e})) \ln\left(\frac{P}{P_{cr}}\right) + 0.2 \qquad \text{(4.1 – copied from Section 4.2)}$$

where the EI_{eff} represents the effective stiffness, EI_o represents the original stiffness of the wall, t represents the wall thickness, e represents the axial load eccentricity, P represents the applied axial load and P_{cr} represents the critical buckling load. It is currently proposed that the applied lateral load be converted into an axial load at a corresponding eccentricity when using Equation 4.1, though this was not verified as part of this thesis.

The equation for calculating the critical buckling load is the following (refer to Equation 1.3 in the “Thesis Overview” chapter for further explanation):

$$P_{cr} = \pi^2 (EI)_{eff} / [(1 + 0.5\beta)(kh)^2]$$

As the critical buckling load itself depends on the value of the effective stiffness, EI_{eff}, an iterative approach must be taken to determine the effective stiffness. It is recommended to start by guessing an EI_{eff} value and iterating until both sides of the equation are equal. Once the secondary moment is calculated using the moment magnifier or the load displacement method, the wall section is then to be designed to resist the applied axial load and the secondary moment.

4.5.2 Slender Wall Design Examples

Walls C3 and C5, built as part of the Hatzinikolas et al. (1978a) testing program (described in Table 3.1), are to be designed as examples.

4.5.2.1 Wall C3 Design Example:

The relevant information for Wall C3 is provided in the table below.

Table 4.3 Wall C3 Design Information, as per Hatzinikolas et al. (1978a)

Wall C3			
Applied Axial Load (Test Failure Load)	P	1110	kN
Axial Load Eccentricity	e	32.3*	mm
Primary Applied Moment Due to Axial Load Eccentricity	M	35.9	kNm
Wall (Block) Thickness	t	194	mm
Wall Stiffness	EI_o	$5.986*10^{12}$	Nmm^2
Wall Height	h	3073	mm
Effective Length Factor	k	1	
Slenderness Ratio	kh/t	15.9	
Steel Reinforcement Area (Corresponding to Three #9 Imperial Bars)	A_s	1934	mm^2

*This axial load eccentricity corresponds to one sixth of the wall thickness (t/6).

Firstly, Wall C3 must be compared to the limits set above in the proposed design procedure to predict its potential failure mode. As there is no applied lateral load, the wall was built to a slenderness ratio of 15.9 (less than 40 as set above) and the axial load eccentricity corresponds to one sixth of the wall's thickness (meeting the above limit), Wall C3 is not expected to experience out-of-plane failure. As such, a secondary moment is not calculated and the applied axial load (1110 kN) and moment due to eccentricity (35.9 kNm) are to be used to design the wall section.

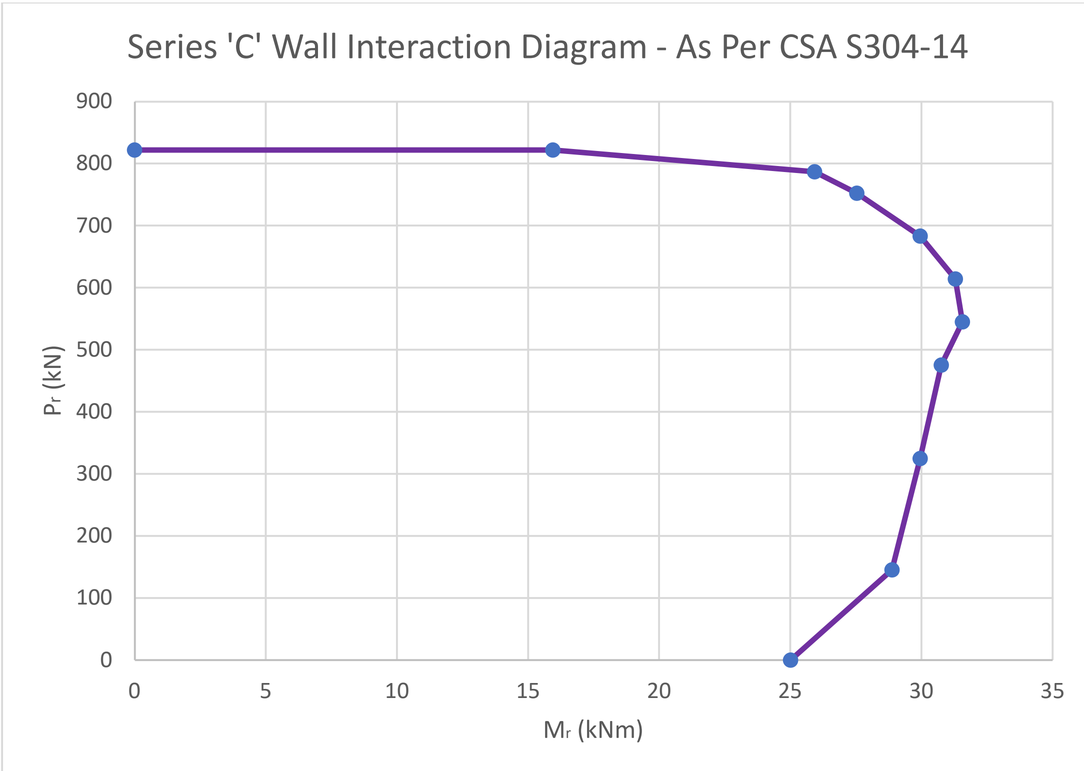

Figure 4.13 Wall Series 'C' Interaction Diagram – As Per CSA S304-14

In the case of Wall C3, 1110 kN was the recorded failure load (causing a corresponding applied moment of 35.9kNm) in the experiment result report (Hatzinikolas et al., 1978b). Once an PM interaction failure envelope is produced, as shown in Figure 4.13, it can be observed that the cross-section of Wall C3 is inadequate to resist the applied load (which is known to have caused the failure). If this wall was being redesigned as per the Canadian Standard to resist the aforementioned failure load, the section thickness, reinforcement ratio or block strength would have to be increased and another corresponding PM interaction diagram produced. It is worth noting that the above-applied loads are very high relative to the typical design loads in industry, as slender walls in typical construction situations must resist relatively low axial loads.

4.5.2.2 Wall C5 Design Example

The relevant information for Wall C5 is provided in the table below.

Table 4.4 Wall C5 Design Information, as per Hatzinikolas et al. (1978a)

Wall C5			
Applied Axial Load (Test Failure Load)	P	545	kN
Axial Load Eccentricity	e	76.2*	mm
Primary Applied Moment Due to Axial Load Eccentricity	M	41.5	kNm
Wall (Block) Thickness	t	194	mm
Wall Stiffness	EI_o	$5.986*10^{12}$	Nmm^2
Wall Height	h	3073	mm
Effective Length Factor	k	1	
Slenderness Ratio	kh/t	15.9	
Steel Reinforcement Area (Corresponding to Three #9 Imperial Bars)	A_s	1934	mm^2

*This axial load eccentricity corresponds to two fifths of the wall thickness (2t/5).

Firstly, Wall C5 must be compared to the limits set above in the proposed design procedure to predict its potential failure mode. As there is no applied lateral load, the wall was built to a slenderness ratio of 15.9 (less than 40 as set above), but the axial load eccentricity corresponds to two fifths of the wall's thickness (exceeding the above limit), Wall C5 is expected to experience out-of-plane failure. As such, a secondary moment is to be calculated. An effective stiffness, EI_{eff}, must first be iterated for and then used to determine the secondary moment using the equation (see proposed design procedure above):

$$\frac{EI_{eff}}{EI_o} = -(0.05 * (\frac{t}{e})) \ln\left(\frac{P}{P_{cr}}\right) + 0.2$$

Note the equation for calculating P_{cr}:

$$P_{cr} = \pi^2 (EI)_{eff} / [(1 + 0.5\beta)(kh)^2]$$

Upon iterating to determine effective stiffness (such that the right and the left side of the equation are equal), the following value is reached:

$EI_{eff} = 1.855*10^{12}$ Nmm^2

Next, the moment magnifier method (load displacement method can also be used) is used to determine the secondary moment (see Equation 1.2 in the “Thesis Overview” chapter):

$$M_{ftot} = M_{fp} \frac{C_m}{1-\frac{P_f}{P_{cr}}}$$

The calculated secondary moment to be used to design the wall section is 72 kNm.

Therefore, the applied axial load (545 kN) and secondary moment (72 kNm) are to be used to design the wall section (see Figure 4.13 for wall section PM interaction diagram). In the case of Wall C5, an applied axial load of 545 kN was the recorded failure load in the experiment result report (Hatzinikolas et al., 1978b), and so the wall cross-section noted in the table above would be inadequate to resist the applied load (which is known to have caused the failure). If this wall was being redesigned as per the Canadian Standard to resist the aforementioned failure load, the section thickness or block strength would have to be increased and a new corresponding PM interaction diagram produced.

4.6 In Conclusion: Further Research Required

This thesis has built on previous research which identified inaccuracies in the Canadian Standard, CSA S304-14 (2014), and further quantitatively assessed the degree to which the Standard is conservative with respect to the design of slender masonry walls. In particular, as presented in the previous “Methodology and Results” chapter, the degree to which the effective stiffness term is being incorrectly calculated has been demonstrated. In the same chapter the incorrect assessment of wall failure mode is noted as an even more significant probable cause of these inaccuracies. Based on the research laid out throughout this chapter, two main recommendations are being proposed which should contribute to a more precise and elegant design procedure for walls which currently meet or exceed the slenderness ratio to be considered walls which experience slenderness effects, as per the Standard.

Walls which meet the slenderness ratio criteria to be designed currently as a wall which experiences slenderness effects (secondary moment effects), as per the Standard, CSA S304-14 (2014), should also be categorized as per their failure modes first, before proceeding with specific design procedures. The research which has been laid out very strongly suggests that considering the slenderness ratio alone is not sufficient in determining the failure mode a particular wall is to experience. An approach such as the one suggested in Section 4.5 would allow for more reasonable and elegant design of walls with high slenderness ratios which are loaded at a low axial load eccentricity, as these walls would typically not be expected to experience flexural or buckling failure, but rather compressive material failure. As per the Alberta Masonry Council (2020), particular applications such as school gymnasia and warehouses where the unbraced wall heights are high are areas of significant overdesign of typically concrete block walls and are leading to masonry being excluded in favour of other construction materials and approaches. As per the results of this study, identifying a wall's failure mode and applying the appropriate design procedure appears to be the single most effective step in reducing the inaccuracy previously inherent in the Canadian Standard, particularly when certain walls were designed to resist secondary moment effects but were typically experiencing material compressive failure. This fact had been overlooked in previous testing programs and had not impacted the Canadian Standard procedure for the design of slender masonry walls, which is why it is identified and particularly highlighted in this thesis as critical understanding which can contribute to the significant reduction of the conservativeness inherent in slender masonry wall design.

It is demonstrated in the previous "Methodology and Results" chapter that the effective stiffness as per the CSA S304-14 (2014) calculation is underestimated even for walls which are truly experiencing secondary moment effects. Thus, lateral displacements and thus secondary moments can be amplified excessively in the design procedure. For walls which fail in flexure, the effective stiffness as per the Standard is more precise for the walls which are loaded at a higher axial load eccentricity, while the effective stiffness calculation is less accurate for the walls loaded at a lower axial load eccentricity. For walls which fail in flexure, a more precise approach to the calculation of the effective stiffness should be applied. As proposed in Section 4.2, an equation that more accurately models the reduction of the cross-sectional area as a wall is loaded should be included in the slender wall design procedure (Equation 4.1). While the equation proposed above seemed to work well for the available data considered in this study, the capability of the equation must be further compared to further testing programs and modelling outcomes with a variety of testing conditions. For instance, the effect wall fixity has on the decrease of the wall's effective stiffness (as well as failure mode) as it is loaded should be explored further. Additionally, walls of varying materials, load conditions (including single and double curvature), end conditions, steel reinforcement ratios and initial imperfections must be assessed to ensure that any design equation is broadly applicable. As the current emphasis on slenderness being the height to thickness ratio is based on research on solid brick walls (where there is a constant relationship between wall thickness and radius of gyration), some consideration should also be given to a return to the more exact definition of slenderness being the ratio of height to radius of gyration. If this were reviewed partially grouted concrete masonry walls could be permitted higher loads than with the current definition.

With respect to both of the above proposed procedural changes to the design of slender masonry walls further study is recommended as certain factors could not be considered as part of this thesis. An experimental program should confirm many of the theoretical results and conclusions from this thesis. Namely, the trends in the effective stiffness values which have been observed as part of this thesis should be confirmed experimentally. As mentioned previously, a wider range of walls of varying slenderness ratios and material properties should be considered. Perhaps the range of results needed could be developed through parametric finite element modelling combined with some validating experimental tests. Notably, this research did not focus as directly on the design of slender walls with a slenderness ratio above 30. As per the Standard, an additional significant (90%) reduction in axial load capacity must be applied to walls which are loaded axially at a slenderness ratio of 30 and over (see clause 10.7.4.6.4 of CSA S304-14 (2014)). This significant reduction is itself a major cause of overdesign, as shown by Ahmed et al. (2021) in the case of slender walls ($kh/t \geq 30$) loaded at a low axial load eccentricity. As part of future research, this provision in the Standard should itself be reviewed with respect to slender walls which are expected to fail in flexure.

Lastly, it is recognized as these recommendations are being made that this research can serve as a theoretical basis for potential changes in the Canadian Standard (of which CSA S304-14 is the most recent iteration), but that this research does not consider the realities of inherent inaccuracies in the construction and material sourcing processes. Therefore, future studies will need to assess the degree of conservativeness which should be embedded in the design procedure of slender masonry walls.

References

ACI-SEASC Task Committee on Slender Walls. 1982. *Test Report on Slender Walls.* ACI Southern California Chapter/Structural Engineers Association of Southern California, Los Angeles, California.

Ahmed, A., Iskander, G., Bogoslavov, M., Isfeld, A., Shrive, N.G. 2021. *Examining the Mode of Failure of Slender Concrete Block Walls*. Proc., 14th Canadian Masonry Symposium, Montreal, Canada.

Banting, B. 2020. Mississauga, Ontario: Canada Masonry Design Centre. (Personal Correspondence)

Bogoslavov, M. and Shrive, N.G. 2020. *The Influence of Effective Flexural Stiffness on Slender Masonry Wall Capacity*. Proc., 17th International Brick and Block Masonry Conference, Krakow, Poland.

Canadian Standards Association. 2004. *S304.1-04 Design of Masonry Structures.* Mississauga, Ontario, Canada: CSA Group.

Canadian Standards Association. 2014. *S304.1-14 Design of Masonry Structures.* Mississauga, Ontario, Canada: CSA Group.

Canadian Wood Council. 2000. *Tall Walls Workbook*, Ottawa, Ontario, Canada.

Hagel, M. 2020. Tall Walls Presentation. Calgary, Alberta: Alberta Masonry Council. (Personal Correspondence)

Hatzinikolas, M., Longworth, J., Warwaruk, J. 1978a. *Concrete Masonry Walls, Structures Report No. 70.* University of Alberta, Edmonton, AB, Canada.

Hatzinikolas, M., Longworth, J., Warwaruk, J. 1978b. *Experimental Data for Concrete Masonry Walls, Structural Engineering Report No.71*. University of Alberta, Edmonton, AB, Canada.

Isfeld, A.C., Müller, A.L., Hagel, M. and Shrive, N.G. 2018. *Analysis of Safety of Slender Concrete Masonry Walls in Relation to CSA S304-14*. Canadian Journal of Civil Engineering, Vol. 46, No. 5, pp.424–438.

Isfeld, A.C., Hagel, M., Shrive, N.G. 2019. *Finite Element Analysis of Hollow Concrete Block Masonry Walls*. Proc., 13th North American Masonry Conference, Salt Lake City, Utah, USA.

Isfeld, A.C., Müller, A.L., Hagel, M. and Shrive, N.G. 2020. *Testing and Finite Element Modelling of Concrete Block Masonry Walls Under Axial and Out-of-Plane Loading*. International Journal of Masonry Research and Innovation, Vol. 6, No. 1, pp.60–80.

Liu, Y., Dawe, J. L. 2003. *Analytical Modeling of Masonry Load-Bearing Walls.* Canadian Journal of Civil Engineering 30, 795-806.

Liu, Y., Hu, K. 2007. *Experimental Study of Reinforced Masonry Walls Subjected to Combined Axial and Out-of-Plane Bending.* Canadian Journal of Civil Engineering 34, 1486-1494.

Müller, A.L., Isfeld, A.C., Hagel, M., Shrive, N.G. 2017. *Review and Analysis of Capacity of Slender Concrete Masonry Walls*. Proc. 13th Canadian Masonry Symp., Halifax, Paper 43, 11pp.

Mohsin, E., Elwi, A. E. 2003. *Effect of Implied Fixity at Masonry Block Wall-Support Interface on Stability of Load Bearing Walls*. North American Masonry Conference, Clemson, South Carolina, USA.

National Research Council of Canada. 2015. *National Building Code of Canada 2015*. Canadian Commission on Building and Fire Codes, Ottawa, ON, Canada.

Ojinaga, J. and Turkstra, C. J. 1980. *The Design of Plain Masonry Walls*. Canadian Journal of Civil Engineering, 7, 233-242.

Ojinaga, J. and Turkstra, C. J. 1982. *Design of Reinforced Masonry Walls and Columns for Gravity Loads.* Canadian Journal of Civil Engineering, 9, 84-95.

Suwalski, P.D. 1986. *Capacity of Eccentrically Loaded Slender Concrete Block Walls.* M. Eng. Thesis, Dept. of Civil Engineering and Engineering Mechanics, McMaster University, Hamilton, Ontario.

Yokel, F. Y., Mathey, R. G., Dikkers, D. R. 1970. *Compressive Strength of Slender Concrete Masonry Walls*. National Bureau of Standards.

Yokel, F. Y., Mathey, R. G., Dikkers, D.R. 1971. *Strength of Masonry Walls Under Compressive and Transverse Loads.* National Bureau of Standards.